



Cite this: DOI: 10.1039/c6dt00990e

Aluminum complexes containing salicylbenzoxazole ligands and their application in the ring-opening polymerization of *rac*-lactide and ϵ -caprolactone†Pattarawut Sumrit,^a Pitak Chuawong,^b Tanin Nanok,^c Tanwawan Duangthongyou^c and Pimpa Hormnirun^{*a}

Two series of four-coordinate aluminum (**1a–9a**) and five-coordinate aluminum (**1b–9b**) complexes were successfully synthesized *via* the reactions between the corresponding salicylbenzoxazole ligands and 1 or 0.5 equivalents of AlMe₃, respectively. The synthesized aluminum complexes were characterized by ¹H and ¹³C NMR spectroscopy and elemental analysis. The solid-state structures of complexes **7a** and **1b** were determined using single crystal X-ray diffraction. Upon addition of 1 equivalent of benzyl alcohol, all complexes were efficient initiators for the ring-opening polymerization (ROP) of *rac*-lactide (*rac*-LA) and ϵ -caprolactone (ϵ -CL). The polymerizations were living with a good control over molecular weights and molecular weight distributions. Under immortal polymerization conditions, all four-coordinate aluminum complexes (**1b–9b**) exhibited a living polymerization with the obtained molecular weights proportional to the ratio of monomer/benzyl alcohol and the PDIs were narrow. Kinetic studies revealed that both *rac*-LA and ϵ -CL polymerizations mediated by all complexes were first-order in monomers. The effects of ligand structure and coordination geometry on the catalytic activity and stereoselectivity were discussed. A good isoselectivity control was achieved for the polymerizations mediated by complexes **4b** ($P_m = 0.75$), **5b** ($P_m = 0.74$), and **9b** ($P_m = 0.74$).

Received 13th March 2016,
Accepted 2nd May 2016

DOI: 10.1039/c6dt00990e

www.rsc.org/dalton

Introduction

Due to the environmental concerns and sustainability issues associated with petroleum-based polymers, the demand for biodegradable polymers has increased significantly in recent years. Polylactide (PLA) and polycaprolactone (PCL) are two well-known biodegradable aliphatic polyesters. They have received much interest as high potential materials for medical and pharmaceutical applications due to their biodegradable and biocompatible properties.¹ Ring-opening polymerization (ROP) of the cyclic esters initiated by metal complexes *via* a coordination–insertion mechanism is the most efficient method to produce aliphatic polyesters with good control

regarding molecular weight, molecular weight distribution, and stereoselectivity.² A number of metal complexes, including Al,³ Y,⁴ Ga,⁵ Zn,⁶ Sn,⁷ Ti,⁸ and lanthanide⁹ complexes, have been developed as efficient initiators for the ROP of lactide (LA) and ϵ -caprolactone (ϵ -CL). The increasing interest in this area is evidenced by the number of reviews recently published.¹⁰

Among the various metal initiators, aluminum complexes are well-suited initiators owing to their strong Lewis acidity and low toxicity.^{10a,11} The catalytic performances of aluminum initiators are influenced by the structure of the ancillary ligand. Most interest was devoted to tetradentate ligands due to the ease of fine-tuning their electronic and steric properties. Many aluminum complexes containing tetradentate ligands, such as Salen,¹² Salan,^{12h,13} and Salalen,¹⁴ have been extensively studied and some of them have displayed excellent stereocontrol in the catalytic ROP of *rac*-LA. In the past decade, the use of bidentate ligands has gained increasing attention. However, low stereoselectivity was observed in the polymerization of *rac*-lactide due to a limited influence of steric hindrance on the ligand structure. Bidentate ligands can bind to the metal center in the form of four-coordinate and five-coordinate geometries. For example, four-coordinate aluminum complexes are stabilized by phenoxy-imine (**I**),^{3e,15}

^aLaboratory of Catalysts and Advanced Polymer Materials, Department of Chemistry and Center of Excellence for Innovation in Chemistry, Faculty of Science, Kasetsart University, Bangkok 10900, Thailand. E-mail: fscipph@ku.ac.th

^bDepartment of Chemistry and Center of Excellence for Innovation in Chemistry, Faculty of Science, and Special Research Unit for Advanced Magnetic Resonance (AMR), Kasetsart University, Bangkok 10900, Thailand

^cDepartment of Chemistry, Faculty of Science, Kasetsart University, Bangkok 10900, Thailand

† Electronic supplementary information (ESI) available. CCDC 1429409 and 1429410. For ESI and crystallographic data in CIF or other electronic format see DOI: 10.1039/c6dt00990e

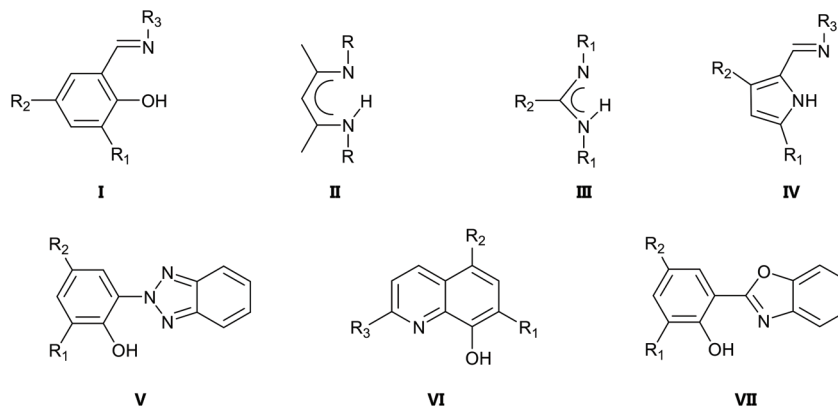


Fig. 1 Structures of monoanionic bidentate ligands.

β -diketiminato (**II**),¹⁶ amidinate (**III**),¹⁷ and other ligands¹⁸ and five-coordinate aluminum complexes are stabilized by pyrrolylaldiminato (**IV**),¹⁹ benzotriazole-phenoxide (**V**)²⁰ and 8-hydroxyquinoline (**VI**) (Fig. 1).^{3b} Besides, aluminum complexes containing other bidentate ligands have been demonstrated to be efficient initiators for the ROP of cyclic esters.²¹

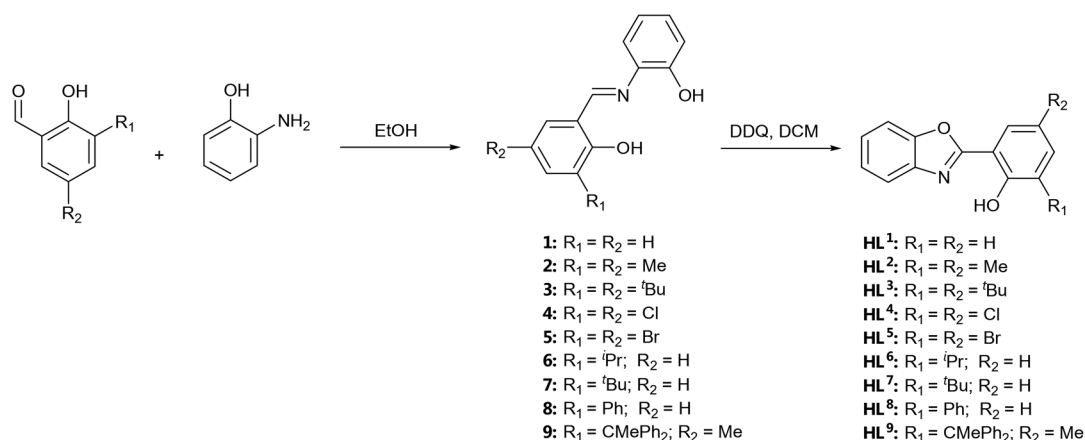
The search for new ancillary ligands is an important key to success for the development of new efficient catalyst systems. The 2-(2'-hydroxyphenyl)benzoxazole (HBO) or salicylbenzoxazole (**VII**) derivatives are an interesting class of ligands due to their strong conjugative effect that might have an influence on the metal center. These ligands were reported to be excellent monoanionic bidentate [N,O] ligands for various metals for the main application as luminescent materials.²² Jin and co-worker reported the synthesis of half-sandwich titanium complexes bearing salicylbenzoxazole ligands for ethylene polymerization.²³ All complexes showed moderate to high activities in the presence of MAO. Recently, the same group designed and synthesized a series of titanium and zirconium salicylbenzoxazole complexes for olefin polymerization.²⁴ The electronic and steric influences on the catalytic activities of zirconium precatalysts were found to be remarkable.

Currently, to the best of our knowledge, there is no report on the use of salicylbenzoxazole aluminum complexes as initiators for the ROP of *rac*-LA and ϵ -CL. Herein, we report the synthesis of a series of four-coordinate and five-coordinate aluminum complexes supported by salicylbenzoxazole ligands, and their catalytic behavior for the polymerizations of *rac*-LA and ϵ -CL.

Results and discussion

Synthesis and characterization of aluminum complexes 1a–9a and 1b–9b

The salicylbenzoxazole proligands **HL**¹–**HL**⁹ were synthesized by a two-step reaction according to a published procedure (Scheme 1).²⁵ The first step is a condensation reaction between 2-aminophenol and the corresponding salicylaldehyde derivative in ethanol to produce compounds 1–9 (see the ESI† for the synthetic procedure), followed by an oxidative cyclization using 2,3-dichloro-5,6-dicyano-1,4-benzoquinone (DDQ) as an oxidant. After purification by column chromatography, the ligands were obtained as off-white solids (11–78%).



Scheme 1 Synthetic route for proligands **HL**¹–**HL**⁹.

The four-coordinate aluminum complexes **1a–9a** were obtained in moderate yields (40–63%) *via* alkane elimination from trimethylaluminum (AlMe₃) and the corresponding proligands in the molar ratio of 1:1 in toluene at room temperature (Scheme 2). Treatment of AlMe₃ with the appropriate proligands in the molar ratio of 1:2 in toluene at 100 °C afforded five-coordinate aluminum complexes **1b–9b** (20–61%). All ligands and aluminum complexes were characterized by ¹H NMR and ¹³C NMR spectroscopy and elemental analysis.

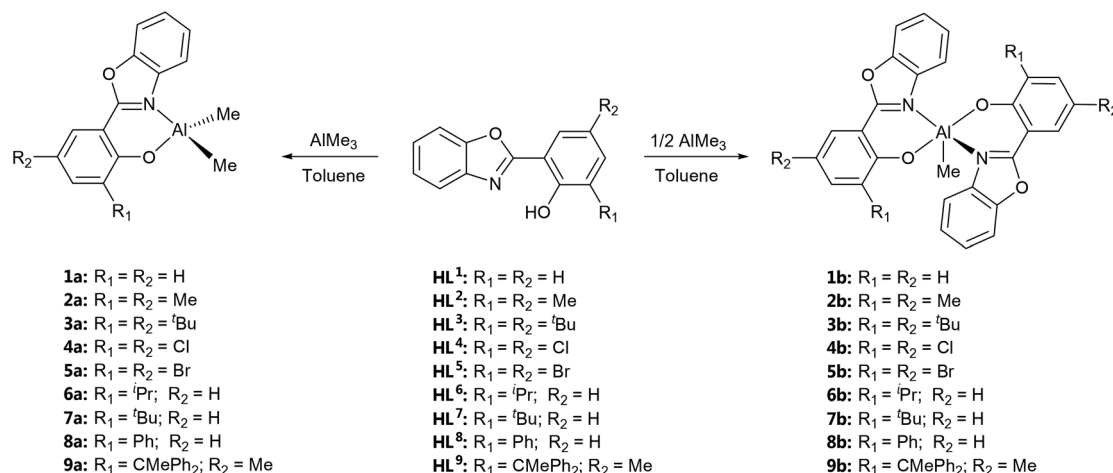
The ¹H and ¹³C NMR spectra of complexes **1a–9a**, **1b–3b** and **5b–9b** in CDCl₃ solution at room temperature contain a single set of resonances, consistent with the existence of a highly symmetric species on the NMR time scale. It is noted that complex **4b** is insoluble in CDCl₃, CD₂Cl₂, C₆D₆, and DMSO-*d*₆ at room temperature. Therefore, the ¹H and ¹³C NMR spectra of **4b** were obtained in toluene-*d*₈ at 70 °C. The disappearance of the O–H signal of the ligand precursors and the appearance of the resonance for the protons of aluminum-methyl groups in the high field region are consistent with the structure proposed in Scheme 2 (see Fig. S2–S19 in the ESI† for the ¹H NMR spectra of the complexes).²⁶ The four-coordinate aluminum complexes **1a–9a** display only one sharp singlet of two magnetically equivalent aluminum methyl groups which can be attributed to the symmetric environment around the aluminum center. For example, the ¹H NMR spectrum of complex **3a** shows the resonance of two methyl groups bound to the aluminum center as a singlet at δ –0.62 ppm. Signals assigned to the *tert*-butyl groups on the phenoxide moiety appeared as two singlets at δ 1.47 and 1.38 ppm. The ¹H NMR spectra for the five-coordinate aluminum complexes are all similar in that both salicylbenzoxazole ligands are magnetically equivalent on the NMR time scale. For example, in complex **3b**, the two aromatic protons from each phenoxide moiety occurred as two doublet resonances at δ 7.88 and 7.40 ppm. Signals ascribed to *tert*-butyl protons appeared as two singlets at δ 1.32 and 0.90 ppm, and the aluminum-methyl resonance was observed at δ –0.11 ppm.

Single crystals of complexes **7a** and **1b** suitable for X-ray diffraction analysis were grown from their DCM/hexane mixed solutions at –20 °C and their molecular structures are illustrated in Fig. 2 and 3, respectively (see Tables S1–S4 in the ESI† for the crystallographic details). The molecular structure of **7a** features a monomeric molecule with a four-coordinate aluminum center in a geometry best described as distorted tetrahedral as seen in the bond angles for O(1)–Al(1)–C(19) [111.99(11)°], N(1)–Al(1)–C(19) [107.97(11)°], O(1)–Al(1)–C(18) [114.56(11)°] and O(1)–Al(1)–N(1) [92.08(9)°] (Fig. 2). The aluminum center coordinated with the phenoxy atom O(1) and the atom N(1) forms a six-membered N,O-chelated ring with co-planarity. The Al–C bond lengths Al(1)–C(18) [1.956(3) Å] and Al(1)–C(19) [1.951(3) Å] are typical.^{15a,b,27} The Al(1)–O(1) bond length is 1.7697(18) Å which is characteristic of σ -bonding^{11a,21b,27} while the Al(1)–N(1) distance is 1.951(2) Å displaying the coordinative covalent bond character.^{11a,21b,27}

Fig. 3 illustrates the molecular structure of the five-coordinate aluminum complex **1b** with a distorted trigonal bipyramidal geometry around the aluminum center. The amount of distortion can be quantified using the geometric criterion $\tau = (\beta - \alpha)/60$.²⁸ The τ value of 0.75 was obtained for complex **1b**, indicating the distorted trigonal bipyramidal character. The diaxial angle, N(2)–Al(1)–N(1), is close to linear [166.35(5)°] and the angles at the aluminum center fall within the narrow range from 119.15(7)° for O(3)–Al(1)–C(27) to 121.02(6)° for O(3)–Al(1)–O(1). The Al–O bond distances [1.787(12) and 1.789(12) Å] and the Al–N bond lengths [2.047(12) and 2.067(13) Å] are similar to those reported in **7a**.

Ring-opening polymerization of *rac*-lactide

The four-coordinate aluminum complexes **1a–9a** and the five-coordinate aluminum complexes **1b–9b** were tested as initiators for the ROP of *rac*-LA in the presence of benzyl alcohol. The *in situ* alcoholysis is a typical protocol for polymerizations employing aluminum initiators.^{3b,12–15} In this study, the formation of the true initiating species was



Scheme 2 Synthetic routes for four-coordinate aluminum complexes (**1a–9a**) and five-coordinate aluminum complexes (**1b–9b**) from HL¹–HL⁹.

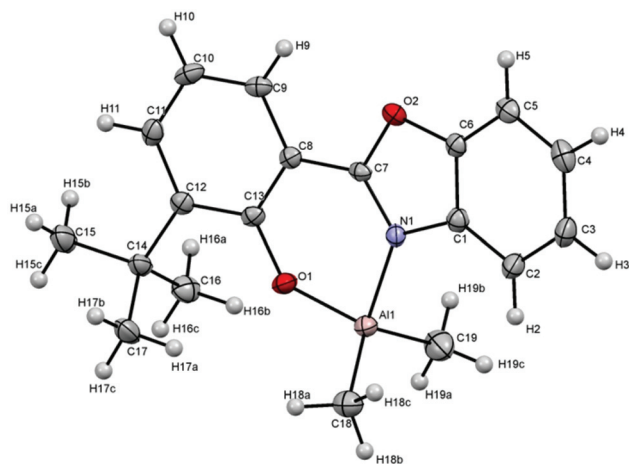


Fig. 2 ORTEP representation of **7a** with the thermal ellipsoids drawn at 50% probability level. Selected bond lengths (Å) and angles (°) are as follows: Al(1)–O(1), 1.7697(18); Al(1)–N(1), 1.951(2); Al(1)–C(19), 1.951(3); Al(1)–C(18), 1.956(3); C(13)–O(1), 1.334(3); C(7)–N(1), 1.317(3); O(1)–Al(1)–N(1), 92.08(9); O(1)–Al(1)–C(19), 111.99(11); N(1)–Al(1)–C(19), 107.97(11); O(1)–Al(1)–C(18), 114.56(11); N(1)–C(7)–C(8), 128.2(2); N(1)–C(7)–O(2), 113.3(2); C(13)–C(8)–C(7), 120.0(2); O(1)–C(13)–C(12), 120.0(2); C(1)–N(1)–Al(1), 131.08(16); C(19)–Al(1)–C(18), 118.06(12).

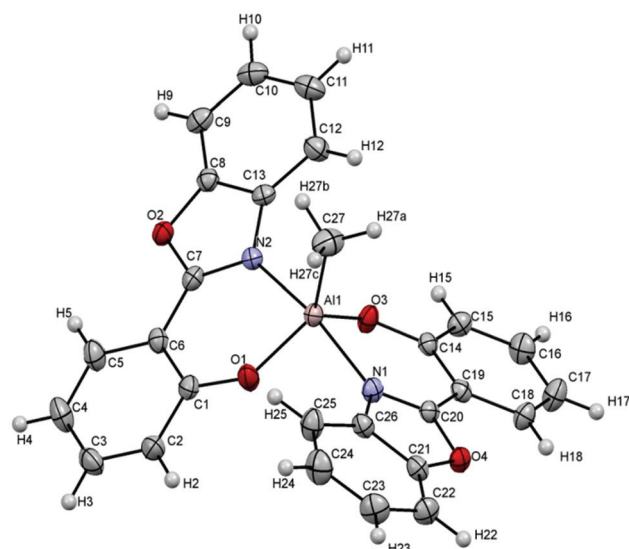


Fig. 3 ORTEP representation of **1b** with the thermal ellipsoids drawn at 50% probability level. A molecule of co-crystallized toluene is omitted for clarity. Selected bond lengths (Å) and angles (°) are as follows: Al(1)–O(3), 1.789(12); Al(1)–N(2), 2.047(12); Al(1)–O(1), 1.787(12); Al(1)–C(27), 1.957(16); Al(1)–N(1), 2.067(13); C(27)–Al(1)–N(2), 98.15(6); N(2)–Al(1)–N(1), 166.35(5); O(3)–Al(1)–O(1), 121.02(6); O(3)–Al(1)–C(27), 119.15(7); O(1)–Al(1)–N(1), 85.15(5); O(3)–Al(1)–N(1), 87.46(5); O(3)–Al(1)–N(2), 85.89(5); O(1)–Al(1)–C(27), 119.79(8); C(27)–Al(1)–N(2), 98.15(6); C(27)–Al(1)–N(1), 95.50(6).

confirmed by a successful synthesis of aluminum benzyloxide complex **10** via a stoichiometric reaction between complex **3b** and benzyl alcohol (see the synthesis and characterization in the ESI and Fig. S20† for the ^1H NMR spectrum). All polymeri-

zations were carried out in toluene at 70 °C. The molar ratio of *rac*-LA to initiator was fixed at 100 : 1 ($[\text{LA}]_0/[\text{Al}] = 100$; $[\text{LA}]_0 = 0.83 \text{ M}$; $[\text{Al}] = 8.33 \text{ mM}$; M_n (theory) = 14 400). The polymerization progress was monitored by taking regular aliquots which were subsequently analyzed by ^1H NMR spectroscopy to determine the conversion. The molecular weights and molecular weight distributions were determined by gel permeation chromatography (GPC) using the Mark–Houwink correction of 0.58.²⁹ The results are summarized in Table 1. The aluminum complexes were all active initiators in the polymerization of *rac*-LA. All of the initiator systems exhibited the molecular weights in good agreement with the theoretical values and narrow molecular weight distributions in accord with controlled living polymerizations (entries 1–18, Table 1). The polymerizations using four-coordinate aluminum complexes **1a–8a** proceeded to ca. 90% within 12 h except the polymerization using complex **9a**, which required 36 h to achieve 88% conversion. For the five-coordinate aluminum complexes **1b–9b**, the polymerizations were relatively slower than those using four-coordinate aluminum analogs. For instance, complexes **3b**, **7b** and **9b** required 144 h to reach 90%, 88% and 90%, respectively. The living characteristic of the polymerization initiated by **1a** was also illustrated by a linear relationship between the number-average molecular weights (M_n) and monomer conversion with narrow molecular weight distributions as shown in Fig. 4.

Polymerizations using four-coordinate aluminum complexes **1a–9a** were also performed under “immortal” conditions,^{3e,15d,30} in which excess benzyl alcohol molecules were added, which acted as a chain transfer agent (CTA). As shown in Table 2, when two equivalents of benzyl alcohol were added (entries 1–9, Table 2), complexes **1a–9a** catalyzed the ROP of *rac*-LA to PLAs with the observed molecular weights close to the theoretical values with narrow PDIs, indicating the living and immortal polymerization. The “immortal” character of all complexes was also observed when increasing the ratio of $[\text{LA}]_0 : [\text{Al}] : [\text{PhCH}_2\text{OH}]$ from 100 : 1 : 2 to 100 : 1 : 10. The molecular weights of the resulting polymers decreased with the M_n value proportional to the monomer/benzyl alcohol ratio, and the molecular weight distributions were still narrow. These results suggested that a fast reversible exchange between dormant hydroxyl-end-capped polymer chains/free alcohol and the active alkoxy-type polymer chain coordinated onto the aluminum center occurred significantly faster than the chain propagation.^{3e,11b,30d} Therefore, the ROP of *rac*-LA mediated by complexes **1a–9a** under “immortal” conditions is an effective method for the synthesis of low molecular weight PLAs using only a small amount of catalyst.

Kinetic studies of *rac*-LA polymerization

Kinetic studies of *rac*-LA polymerization initiated by complexes **1a–9a** and **1b–9b** in the presence of one equivalent of benzyl alcohol were conducted in toluene at 70 °C ($[\text{LA}]_0/[\text{Al}] = 50$; $[\text{Al}] = 8.33 \text{ mM}$; $[\text{LA}]_0 = 0.42 \text{ M}$). Conversions of *rac*-LA over time were monitored by taking regular aliquots which were then analyzed by ^1H NMR spectroscopy. The semilogarithmic plots

Table 1 Polymerization of *rac*-LA using complexes **1a–9a** and **1b–9b** in the presence of benzyl alcohol^a

Entry	Complex	Time (h)	Conv. ^b (%)	M_n (theory) ^c (g mol ⁻¹)	M_n (GPC) ^d (g mol ⁻¹)	M_w/M_n ^d	P_m ^e	k_{app} ^f (10 ⁵ s ⁻¹)
1	1a	12	91	13 200	13 500	1.23	0.60	6.0 ± 0.1
2	1b	36	90	13 100	12 500	1.19	0.71	1.7 ± 0.1
3	2a	12	90	13 100	12 800	1.23	0.54	5.8 ± 0.2
4	2b	72	95	13 800	14 300	1.14	0.71	1.1 ± 0.1
5	3a	12	90	13 100	11 000	1.10	0.68	5.6 ± 0.2
6	3b	144	90	13 100	13 000	1.05	0.67	0.52 ± 0.01
7	4a	12	92	13 400	12 400	1.25	0.54	8.0 ± 0.4
8	4b	36	92	13 400	12 200	1.06	0.75	3.5 ± 0.2
9	5a	12	92	13 400	12 000	1.12	0.55	8.3 ± 0.3
10	5b	36	92	13 400	13 500	1.16	0.74	3.6 ± 0.1
11	6a	12	89	12 900	10 000	1.22	0.54	5.7 ± 0.1
12	6b	36	84	12 200	11 000	1.11	0.67	1.4 ± 0.1
13	7a	12	86	12 500	11 200	1.20	0.69	5.6 ± 0.1
14	7b	144	88	12 800	10 900	1.06	0.64	0.54 ± 0.01
15	8a	12	90	13 100	11 300	1.23	0.55	7.8 ± 0.2
16	8b	36	87	12 600	11 900	1.16	0.71	2.5 ± 0.1
17	9a	36	88	12 800	12 500	1.14	0.70	2.6 ± 0.1
18	9b	144	90	13 100	11 100	1.04	0.74	0.78 ± 0.01

^a $[LA]_0/[Al] = 100$, $[Al]/[PhCH_2OH] = 1$, $[LA]_0 = 0.83$ M, $[Al] = 8.33$ mM, toluene, 70 °C. ^b As determined *via* integration of the methine resonances (¹H NMR) of LA and PLA (CDCl₃, 500 MHz). ^c Calculated by $[(LA]_0/[Al]) \times 144.13 \times \text{conversion}] + 108.14$. ^d Determined by gel permeation chromatography (GPC) calibrated with polystyrene standards in THF and corrected by a factor of 0.58 for PLA. ^e P_m is the probability of the *meso* linkage between monomer units and was calculated from the homonuclear decoupled ¹H NMR spectra of the obtained poly(*rac*-LA): $[mmmm] = P_m^2 + (1 - P_m)P_m/2$; $[mrmr] = [rmmm] = (1 - P_m)P_m/2$; $[rrmr] = (1 - P_m)^2/2$; $[mrrm] = [(1 - P_m)^2 + (1 - P_m)P_m]/2$. ^f $[LA]_0/[Al] = 50$, $[Al]/[PhCH_2OH] = 1$, $[LA]_0 = 0.42$ M, $[Al] = 8.33$ mM, toluene, 70 °C.

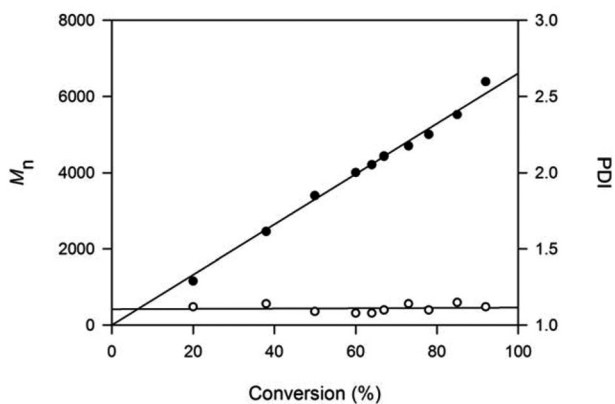


Fig. 4 Plot of PLA M_n (●) (versus polystyrene standards) and PDI (○) as a function of monomer conversion for a *rac*-LA polymerization using **1a**/PhCH₂OH ($[LA]_0/[Al] = 50$, toluene, 70 °C).

of $\ln [LA]_0/[LA]_t$ versus time for the polymerizations using **1a** and **1b** are shown in Fig. 5 (see also Fig. S21–S28 in the ESI† for the plots of other complexes). In all cases, the semilogarithmic plots are linear and intercept the origin, indicating that the polymerizations are first-order in monomer concentration and proceed without an induction period. The absence of an induction period indicated that the polymerization took place immediately after the active aluminum alkoxide species was generated *via in situ* alcoholysis between the aluminum methyl complex and benzyl alcohol. Therefore, the polymerization rate law can be expressed as $-d[LA]/dt = k_{app}[LA]$, where $k_{app} = k_p[Al]^x$, in which k_p is the propagation rate constant. To determine the order in aluminum (x), polymerizations with various

concentrations of the catalyst were performed. For example, the semilogarithmic plots of *rac*-LA conversions versus time for the polymerizations using six different concentrations of **1a** are shown in Fig. 6. The gradient obtained from the plot of $\ln k_{app}$ and $\ln [Al]$ was equal to 1.07 (*ca.* 1.0), signifying a first-order dependence on the aluminum concentration (Fig. 7). In addition, the propagation rate constant (k_p) of $7.38 \times 10^{-3} \text{ s}^{-1} \text{ mol}^{-1} \text{ L}$ was obtained from the slope of the plot between k_{app} and **1a** (Fig. 8). Thus, for the **1a**/PhCH₂OH system, the overall rate equation is $-d[LA]/dt = k_p[LA][1a]$. The same treatment was applied to the determination of the overall rate expression of the **1b**/PhCH₂OH system (see Fig. S29–S31 in the ESI†). The order x was equal to 1.05 (*ca.* 1.0) and the k_p value of $2.22 \times 10^{-3} \text{ s}^{-1} \text{ mol}^{-1} \text{ L}$ was determined. Therefore, the overall rate law in the form of $-d[LA]/dt = k_p[LA][1b]$ was established.

Based on the overall rate law, there are two species involved stoichiometrically in the polymerization process, *i.e.* the active aluminum benzyloxy complex and the lactide monomer. Therefore, the ROP of *rac*-LA follows a monometallic coordination–insertion mechanism with the coordination of *rac*-LA to the aluminum center followed by the ring-opening process.

The apparent rate constants (k_{app}) of all complexes determined from the gradient of $\ln [LA]_0/[LA]_t$ versus time plots are collected in Table 1. It can be seen that the catalytic activity of each four-coordinate aluminum complex was higher than that of its five-coordinate aluminum analog. This can be explained by an increase in steric congestion at the aluminum center when two ligands bind to the metal. For example, the largest difference in catalytic activity was observed for complexes **7a** and **7b** in which the k_{app} value of **7a** ($(5.6 \pm 0.1) \times 10^{-5} \text{ s}^{-1}$) was *ca.* 10 times higher than that of **7b** ($(0.54 \pm 0.1) \times 10^{-5} \text{ s}^{-1}$).

Table 2 Polymerization of *rac*-LA using complexes **1a–9a** in the presence of benzyl alcohol^a

Entry	Complex	[LA] ₀ :[Al]: [PhCH ₂ OH]	Time (h)	Conv. ^b (%)	M _n (theory) ^c (g mol ⁻¹)	M _n (GPC) ^d (g mol ⁻¹)	M _w /M _n ^d
1	1a	100:1:2	8	92	6700	6500	1.20
2	2a	100:1:2	8	90	6600	6500	1.19
3	3a	100:1:2	8	80	5900	5800	1.08
4	4a	100:1:2	8	95	7000	6600	1.18
5	5a	100:1:2	8	91	6700	6200	1.14
6	6a	100:1:2	8	87	6400	6100	1.14
7	7a	100:1:2	8	80	5900	5400	1.08
8	8a	100:1:2	8	88	6400	6200	1.15
9	9a	100:1:2	24	88	6400	6100	1.08
10	1a	100:1:5	8	86	2600	2300	1.19
11	2a	100:1:5	8	71	2100	1700	1.13
12	3a	100:1:5	8	77	2300	2000	1.17
13	4a	100:1:5	8	90	2700	2400	1.06
14	5a	100:1:5	8	90	2700	2300	1.10
15	6a	100:1:5	8	70	2100	2100	1.12
16	7a	100:1:5	8	79	2400	2200	1.11
17	8a	100:1:5	8	90	2700	2500	1.16
18	9a	100:1:5	24	84	2400	2200	1.11
19	1a	100:1:10	8	93	1400	1200	1.16
20	2a	100:1:10	8	77	1200	1100	1.16
21	3a	100:1:10	8	85	1300	1100	1.14
22	4a	100:1:10	8	91	1400	1300	1.13
23	5a	100:1:10	8	81	1300	1100	1.10
24	6a	100:1:10	8	74	1200	1100	1.13
25	7a	100:1:10	8	80	1300	1200	1.15
26	8a	100:1:10	8	80	1300	1100	1.16
27	9a	100:1:10	24	84	1300	1100	1.13

^a [LA]₀/[Al] = 100, [LA]₀ = 0.83 M, [Al] = 8.33 mM, toluene, 70 °C. ^b As determined *via* integration of the methine resonances (¹H NMR) of LA and PLA (CDCl₃, 500 MHz). ^c Calculated by $(\frac{[LA]_0}{[Al]} \times 144.13 \times \text{conversion}) / [\text{PhCH}_2\text{OH}] + 108.14$. ^d Determined by gel permeation chromatography (GPC) calibrated with polystyrene standards in THF and corrected by a factor of 0.58 for PLA.

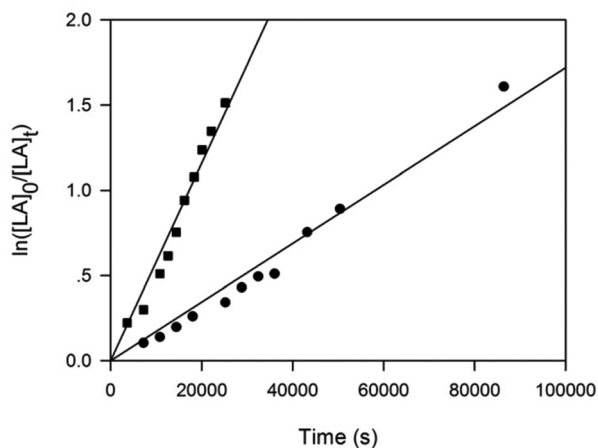


Fig. 5 Semilogarithmic plots of *rac*-lactide conversion versus time in toluene at 70 °C with complexes **1a** (■) and **1b** (●) ([LA]₀/[Al] = 50, [Al]/[PhCH₂OH] = 1, [LA]₀ = 0.42 M, [Al] = 8.33 mM).

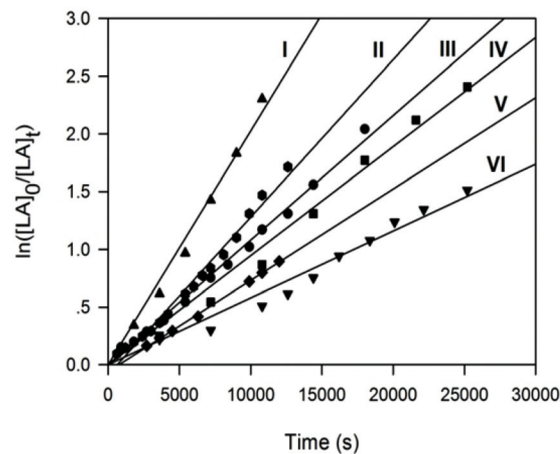


Fig. 6 Semilogarithmic plots of the *rac*-lactide conversion versus time in toluene at 70 °C with complex **1a**/PhCH₂OH as an initiator ([LA]₀ = 0.42 M: I, [Al] = 24.99 mM, [LA]₀/[Al] = 17; II, [Al] = 20.82 mM, [LA]₀/[Al] = 20; III, [Al] = 16.66 mM, [LA]₀/[Al] = 25; IV, [Al] = 12.50 mM, [LA]₀/[Al] = 34; V, [Al] = 10.41 mM, [LA]₀/[Al] = 40; VI, [Al] = 8.33 mM, [LA]₀/[Al] = 50).

It was also found that the catalytic activity decreased when the size of the alkyl phenoxy substituents at the *ortho*- and *para*-positions increased from H to Me to ^tBu, *i.e.* the k_{app} values diminished in the order **1** (H) > **2** (Me) > **3** (^tBu) (entries 1–6, Table 1). Additionally, when the chlorine atoms were introduced at the *ortho*- and *para*-positions of the phenoxy ring (complexes **4a** and **4b**), the catalytic activities of these

complexes (entries 7 and 8, Table 1) were higher than those of their dimethyl substituted counterparts (**2a** and **2b**), suggesting an increase in Lewis acidity at the aluminum center *via* the incorporation of electron withdrawing substituents.³¹

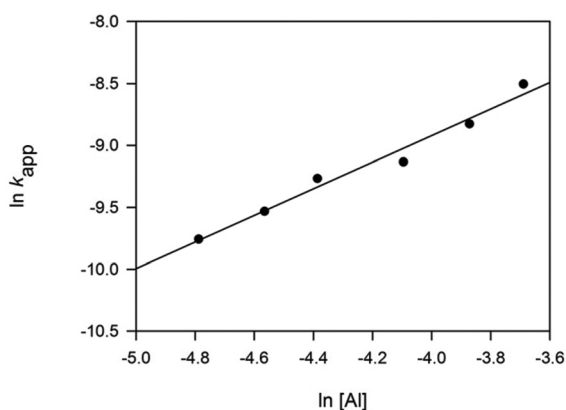


Fig. 7 Plot of $\ln k_{\text{app}}$ versus $\ln [\text{Al}]$ for the polymerization of *rac*-lactide with complex **1a**/ PhCH_2OH as an initiator (toluene, 70 °C, $[\text{LA}]_0 = 0.42 \text{ M}$).

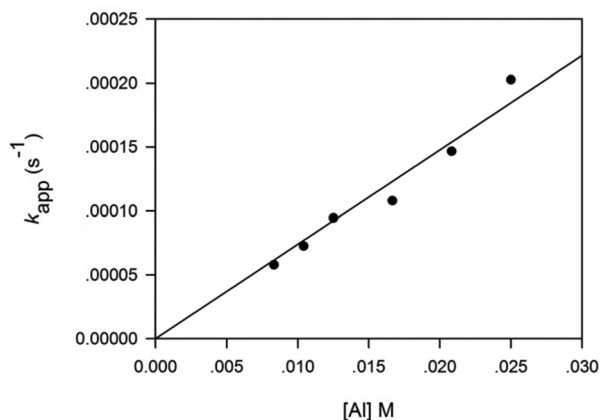


Fig. 8 Plot of k_{app} versus $[\text{Al}]$ for the polymerization of *rac*-lactide with complex **1a**/ PhCH_2OH as an initiator (toluene, 70 °C, $[\text{LA}]_0 = 0.42 \text{ M}$).

However, replacing the dichloro substituents with the less electronegative dibromo atoms (complexes **5a** and **5b**) resulted in a slight increase of activity (entries 9 and 10, Table 1). An increase in catalytic activity as the halogen substituent becomes less electronegative was also observed in other systems.³² This was attributed to the different sensitivities between the coordination and insertion steps to the Lewis acidity of the metal center.³³ The increased Lewis acidity caused by electron withdrawing substituents may result in stronger lactide coordination and activation, but it may also induce stronger binding of the growing alkoxide chain to the metal, decelerating the subsequent insertion step. In addition, the effect of *ortho*- and *para*-substituents on the phenoxy ring was also studied. In comparison with the di-*tert*-butyl substituted complexes (**3a** and **3b**), the catalytic activities of the *ortho-tert*-butyl substituted complexes (**7a** and **7b**, respectively) were comparable (entries 13 and 14, Table 1). These results demonstrated that the steric factor from the *para*-substituent has no significant impact on the catalytic performance of the

catalysts. Despite having the same H substituted atom at the *para*-position of the phenoxy ring, the catalytic activity of complexes **6–8** decreased in the order **8** > **6** > **7** which corresponded to the increase of steric bulkiness from Ph (**8**) to *t*Pr (**6**) to *t*Bu (**7**) (entries 11–16, Table 1). Introducing the more sterically congested CMePh₂– moiety to the *ortho*-position (complexes **9a** and **9b**) appeared to reduce the catalytic activity (entries 17 and 18, Table 1). For the four-coordinate aluminum complexes **1a–9a**, the activities decreased in the order **5a** > **4a** > **8a** > **1a** > **2a** > **6a** > **3a** ≈ **7a** > **9a** while the activities of five-coordinate aluminum counterparts **1b–9b** followed the order **5b** > **4b** > **8b** > **1b** > **6b** > **2b** > **9b** > **3b** ≈ **7b**. The highest catalytic activity in this study was obtained from complex **5a** with a k_{app} value of $(8.3 \pm 0.3) \times 10^{-5} \text{ s}^{-1}$, whereas complex **3b** displayed the lowest k_{app} value $(0.52 \pm 0.01) \times 10^{-5} \text{ s}^{-1}$.

Stereoselectivity of *rac*-LA polymerization

The polymer microstructures of the PLAs were determined by the inspection of the methine region of the homonuclear decoupled ¹H NMR spectra of the resultant polymers.³⁴ All homonuclear decoupled ¹H NMR spectra produced by complexes **1a–9a** and **1b–9b** are shown in Fig. S32–S49.† All initiators gave rise to PLA which has some degrees of isotactic enchainment. In comparison, the degree of isoselectivity of five-coordinate aluminum complexes **1b–9b** ($P_m = 0.64–0.75$) was higher than that of four-coordinate aluminum analogs **1a–9a** ($P_m = 0.54–0.70$). The lower stereoselectivity observed in the four-coordinate aluminum complexes can be attributed to the large coordination sphere for the lactide to coordinate to the aluminum center, which leads to a decrease in the catalyst's ability to select the desired stereoisomer of the lactide. In the cases of four-coordinate aluminum complexes, it is apparent that the isoselectivity increases with the steric encumbrance of the *ortho* phenoxy substituent. Complexes **3a** (*o*-*t*Bu), **7a** (*o*-*t*Bu), and **9a** (*o*-CMePh₂) produced moderate isotactic PLAs with the P_m values of 0.68, 0.69, and 0.70, respectively while the other complexes in the series polymerized *rac*-LA with a slight isotactic bias ($P_m = 0.54–0.60$). In the series of five-coordinate aluminum complexes, the variation of the *ortho* substituent at the phenoxy ring has no influence on the stereoselectivity. The isotactic-enriched PLAs were produced by complexes **4b** ($P_m = 0.75$), **5b** ($P_m = 0.74$), and **9b** ($P_m = 0.74$) as evidenced by the observed strong mmm peak illustrated in Fig. S39, S41 and S49,† respectively. In addition, the influence of polymerization temperature on the degree of isoselectivity was investigated using complex **4b**. It was found that the degree of isoselectivity increased with the decrease of the polymerization temperature from 70 °C to 50 °C ($[\text{LA}]_0/[\text{Al}]/[\text{PhCH}_2\text{OH}] = 100/1/1$, $[\text{Al}] = 8.33 \text{ mM}$, toluene, 168 h, 96% conversion, $M_n = 14\,900$, PDI = 1.03). A highly isotactic PLA with a P_m value of 0.80 was produced (see Fig. S50 in the ESI†).

In general, the stereoselectivity control cannot be achieved directly from a bidentate ligand system due to a restricted influence of steric hindrance. Therefore, it is noteworthy that these bidentate aluminum complexes (**4b**, **5b**, and **9b**) can produce isotactic PLAs that are among the highest reported so

far for these type of aluminum complexes.^{3b,e,8f,19a} For example, the aluminum complexes supported by 8-hydroxyquinoline ligands (**VI**) produced isotactic-biased PLAs with the highest P_m values of 0.70–0.76.^{3b,8f} The dialkylaluminum complexes stabilized by phenoxy-imine ligands (**I**) gave rise to PLAs with different degrees of selectivity ($P_m = 0.29$ –0.80).^{8f} For aluminum pyrrolylaldimine complexes (**IV**), the highest P_m value of 0.74 was reported.^{19a}

Ring-opening polymerization of ϵ -caprolactone

The ring-opening polymerizations of ϵ -caprolactone using all aluminum complexes (**1a–9a** and **1b–9b**) were also investigated under identical conditions for the polymerization of *rac*-LA. The results are summarized in Table 3. The molecular weights and molecular weight distributions were determined by gel permeation chromatography (GPC) using the Mark–Houwink correction factor of 0.56.³⁵ All complexes were found to be active initiators. GPC analysis of the PCL samples obtained from all complexes displayed monomodal molecular weight distributions ranging from 1.02–1.56. The number-average molecular weights were in good agreement with the theoretical values, indicating the single-site nature of these initiators. Similar to the ROP of *rac*-LA, the four-coordinate aluminum complexes (**1a–9a**) exhibited higher catalytic activity than their five-coordinate aluminum counterparts (**1b–9b**). As shown in Table 3, the polymerizations using complexes **1a–9a** proceeded to more than 99% monomer conversion within 15 min whereas a longer polymerization time was required for the polymerization using complexes **1b–9b**. The polymerizations using complexes **3b**, **7b**, and **9b** required 180 min to reach >99% conversion. Complexes **1b**, **2b**, and **6b** polymerized *rac*-LA to >99% conversion within 120 min whereas complexes **4b**,

5b, and **8b** were much more active and reached completion in 30 min.

Kinetic studies of ϵ -CL polymerization

The kinetics of the ROP of ϵ -CL initiated by complexes **1a–9a** and **1b–9b** in the presence of one equivalent of benzyl alcohol were studied in more detail. The polymerizations were carried out in C_6D_6 at 40 °C and the molar ratio of $[\epsilon\text{-CL}]_0/[Al]/[PhCH_2OH]$ was fixed at 50/1/1 ($[Al] = 16.67$ mM; $[\epsilon\text{-CL}]_0 = 0.83$ M). The conversion of ϵ -CL was monitored by 1H NMR spectroscopy and the semilogarithmic plots of $\ln([\epsilon\text{-CL}]_0/[\epsilon\text{-CL}]_t)$ versus time for the polymerizations using **1a** and **1b** are shown in Fig. 9 (see also Fig. S51–S58 in the ESI† for the plots of

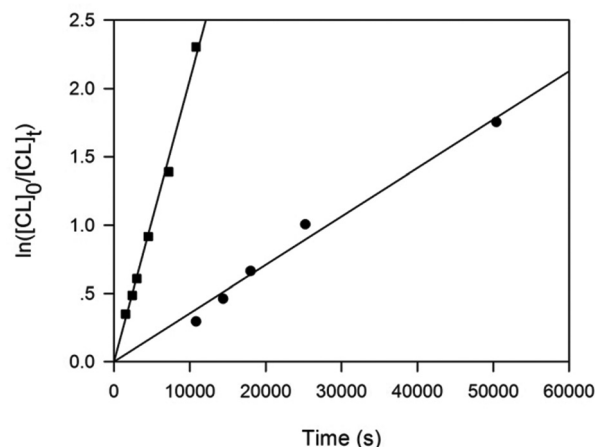


Fig. 9 Semilogarithmic plots of *rac*-lactide conversion versus time in C_6D_6 at 70 °C with complexes **1a** (■) and **1b** (●) ($[\epsilon\text{-CL}]_0/[Al] = 50$, $[Al]/[PhCH_2OH] = 1$, $[\epsilon\text{-CL}]_0 = 0.83$ M, $[Al] = 16.67$ mM).

Table 3 Polymerization of ϵ -caprolactone using complexes **1a–9a** and **1b–9b** in the presence of benzyl alcohol^a

Entry	Complex	Time (min)	Conv. ^b (%)	M_n (theory) ^c (g mol ⁻¹)	M_n (GPC) ^d (g mol ⁻¹)	PDI ^d	k_{app} ^e (10 ⁴ s ⁻¹)
1	1a	15	>99	11 500	14 500	1.47	2.1 ± 0.1
2	1b	120	>99	11 500	11 600	1.54	0.4 ± 0.1
3	2a	15	>99	11 500	10 600	1.42	4.2 ± 0.3
4	2b	120	>99	11 500	10 000	1.19	1.0 ± 0.1
5	3a	15	>99	11 500	13 400	1.56	4.5 ± 0.1
6	3b	180	>99	11 500	12 500	1.35	0.6 ± 0.1
7	4a	15	>99	11 500	13 000	1.28	5.2 ± 0.3
8	4b	30	>99	11 500	10 600	1.07	1.5 ± 0.1
9	5a	15	>99	11 500	12 200	1.29	12.0 ± 0.1
10	5b	30	>99	11 500	12 400	1.02	1.4 ± 0.1
11	6a	15	>99	11 500	12 600	1.17	3.8 ± 0.2
12	6b	120	>99	11 500	12 400	1.21	0.9 ± 0.1
13	7a	15	>99	11 500	11 300	1.42	4.7 ± 0.2
14	7b	180	>99	11 500	11 000	1.40	0.6 ± 0.1
15	8a	15	>99	11 500	11 900	1.54	5.9 ± 0.3
16	8b	30	>99	11 500	10 600	1.14	1.9 ± 0.1
17	9a	15	>99	11 500	9500	1.24	3.8 ± 0.2
18	9b	180	>99	11 500	9400	1.04	0.6 ± 0.1

^a $[\epsilon\text{-CL}]_0/[Al] = 100$, $[Al]/[PhCH_2OH] = 1$, $[\epsilon\text{-CL}]_0 = 1.67$ M, $[Al] = 16.7$ mM, toluene, 70 °C. ^b As determined via integration of the methylene resonances (1H NMR) of ϵ -CL and PCL ($CDCl_3$, 500 MHz). ^c Calculated by $[(\epsilon\text{-CL})_0/[Al]] \times 114.13 \times \text{conversion}] + 108.14$. ^d Determined by gel permeation chromatography (GPC) calibrated with polystyrene standards in THF and corrected by a factor of 0.56 for PCL. ^e $[\epsilon\text{-CL}]_0/[Al] = 50$, $[Al]/[PhCH_2OH] = 1$, $[\epsilon\text{-CL}]_0 = 0.83$ M, $[Al] = 16.67$ mM, C_6D_6 , 40 °C.

other complexes). In all cases, the polymerization followed first-order kinetics in ϵ -CL concentrations and no induction period was observed, indicating that the active species formed instantaneously by an *in situ* alcoholysis reaction. In addition, the living character of the polymerization process was demonstrated by a linear increase of the M_n values with monomer conversion and the observed narrow molecular weight distributions, as illustrated in Fig. 10 (see also Fig. S59 in the ESI†).

The apparent first-order rate constants (k_{app}) are collected in Table 3. For the four-coordinate aluminum complexes **1a**–**9a**, the k_{app} values followed the order **5a** > **8a** > **4a** > **7a** > **3a** >

2a > **6a** \approx **9a** > **1a**. In the cases of the five-coordinate aluminum complexes, the catalytic activity decreased in the order **8b** > **4b** > **5b** > **2b** > **6b** > **3b** \approx **7b** \approx **9b** > **1a**. To a certain extent, the trend can be understood on the basis of steric and electronic considerations. The presence of electron-withdrawing groups at the *ortho*- and *para*- positions of the phenoxy ring resulted in an increase of catalytic activity whereas a diminished catalytic activity was observed by increasing steric bulkiness at the *ortho*- and *para*- positions of the phenoxy ring. For instance, the low k_{app} value of $(0.6 \pm 0.1) \times 10^{-4} \text{ s}^{-1}$ was obtained for the polymerizations using complexes **3b** (*t*Bu), **7b** (*t*Bu), and **9b** (CMePh₂) with the bulky *ortho*-phenoxy substituent. In each series of aluminum complexes, complexes **1a** and **1b** showed the lowest k_{app} value. Given the unsubstituted phenoxy moiety, the decrease in the catalytic activity was rather unexpected. Further studies will be required to understand these observations.

End-group analysis by ¹H NMR spectroscopy

In order to investigate the polymerization mechanism, end-group analyses of the low molecular weight polymer samples were performed using ¹H NMR spectroscopy. Fig. 11 and 12 show the ¹H NMR spectra of PLA-40 and PCL-40, respectively (number 40 indicates the designed [LA]₀/[Al] or [ε-CL]₀/[Al] = 40). According to the ¹H NMR spectrum of PLA-40, the polymer chain is capped with a benzyl ester group on one end and a hydroxyl group on the other end with the integration ratio of H_e : H_c = 5 : 1 (H_c = –CH(CH₃)OH; H_e = –OCH₂C₆H₅). These results indicated that the back-biting reaction leading to the formation of cyclic polyesters did not take place and the

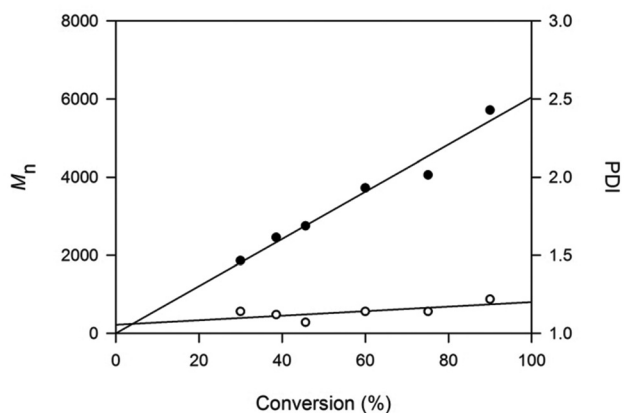


Fig. 10 Plot of PLA M_n (●) (versus polystyrene standards) and PDI (○) as a function of monomer conversion for a ϵ -CL polymerization using **1a**/PhCH₂OH ([ϵ -CL]₀/[Al] = 50, C₆D₆, 40 °C).

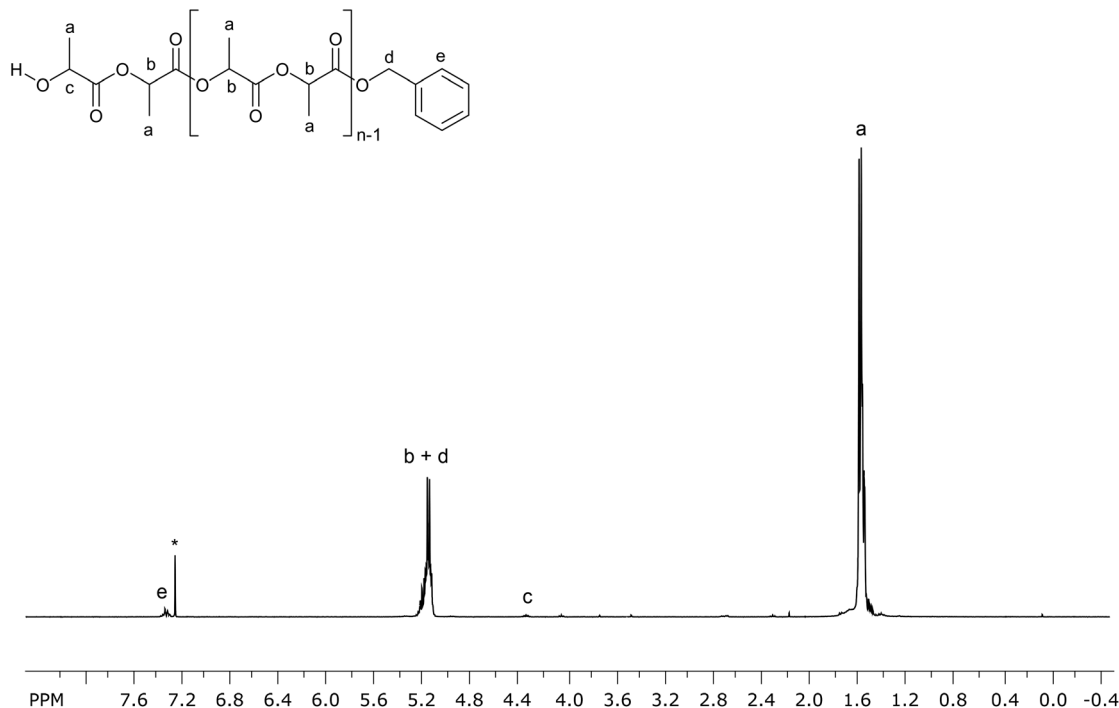


Fig. 11 ¹H NMR spectrum of PLA-40 initiated by **1b** in CDCl₃ at 298 K (* = solvent residue peak).

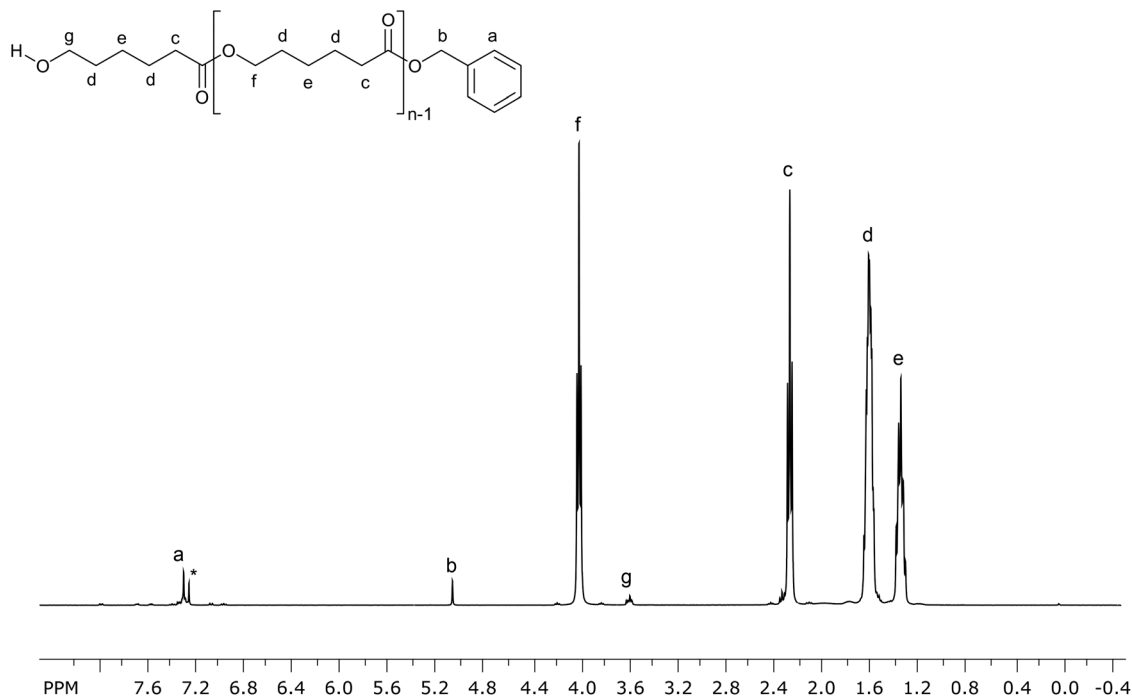


Fig. 12 ^1H NMR spectrum of PCL-40 initiated by **1b** in CDCl_3 at 298 K (* = solvent residue peak).

ring-opening of *rac*-LA occurred *via* an acyl-oxygen bond. In the case of PCL-40, the ^1H NMR spectrum displays an integration ratio close to 1 between H_b ($-\text{OCH}_2\text{Ph}$) and H_g ($-\text{CH}_2\text{OH}$), signifying that the polymer chain is also capped with one benzyl ester and one hydroxyl end. This observation implied that the terminal alkoxide OCH_2Ph was the initiating group in the polymerization process. Thus, a coordination-insertion mechanism, proceeding through acyl-oxygen cleavage of the monomer, should be operative in this system.

Conclusions

In conclusion, two series of aluminum complexes supported by salicylbenzoxazole ligands (complexes **1a–9a** and **1b–9b**) were successfully synthesized and characterized. All complexes were found to be effective initiators for the polymerizations of *rac*-LA and ϵ -CL in the presence of benzyl alcohol. A linear correlation between M_n and percentage conversion was observed, and the PDI values were narrow throughout the polymerization. An effective immortal polymerization was achieved when excess alcohol was added. Kinetic studies revealed that the four-coordinate aluminum complex exhibited higher activity than its five-coordinate counterpart. An increase of steric bulk at the *ortho* phenoxy substituent resulted in a decrease in catalytic activity while the substitution with an electron withdrawing halogen atom at the *ortho* position exerted higher activity. Analysis of polymer microstructure revealed that more isoselectivity control was achieved in the five-coordinate aluminum complexes. For the series of four-coordinate aluminum complexes, the steric encumbrance at

the *ortho* phenoxy position increased the degree of isoselectivity at the metal center. End-group analyses of the low molecular weight polymers verified that the polymerizations of *rac*-LA and ϵ -CL followed a coordination-insertion mechanism. The influence of the ligand substituent and the metal coordination geometry over the catalytic activity and stereochemistry found in this system could be useful for the development of new metal complexes containing monoanionic bidentate ligands in the future.

Experimental section

Materials and methods

All the manipulations with air- and/or water-sensitive compounds were carried out under a dry nitrogen atmosphere using standard Schlenk and cannula techniques in oven-dried glassware or in a glove box. Toluene and hexane were distilled from Na-benzophenone and CaH_2 prior to use, respectively. Benzyl alcohol was dried over sodium and then freshly distilled onto activated 4 Å molecular sieves. All the solvents were degassed before use, unless stated otherwise. The NMR solvents were dried over 4 Å molecular sieves and degassed prior to use. A 2.0 M solution of trimethylaluminum in toluene (Aldrich) was used without purification. 2-hydroxybenzaldehyde (98%), 3,5-dichloro-2-hydroxybenzaldehyde (99%), 3,5-dibromo-2-hydroxybenzaldehyde (98%), 3,5-di-*tert*-butyl-2-hydroxybenzaldehyde (99%), 2-aminophenol (99%) and 2,3-dichloro-5,6-dicyano-1,4-benzoquinone (98%) were purchased from Aldrich and used as received. 3,5-dimethyl-2-hydroxybenzaldehyde, 3-phenyl-2-hydroxybenzaldehyde, 3-isopropyl-

2-hydroxybenzaldehyde and 3-*tert*-butyl-2-hydroxybenzaldehyde were synthesized using a standard method described in the literature.³⁶ The procedure for preparation of 3-(1,1-diphenylethyl)-5-methyl-2-hydroxybenzaldehyde is provided in the ESI.† *rac*-Lactide (Aldrich) was sublimed three times prior to use. ϵ -Caparolactone (Aldrich) was distilled from CaH₂. All other chemicals are commercially available and were used as received unless otherwise stated. ¹H NMR (500.13 MHz) and ¹³C NMR (125.77 MHz) spectra and the homonuclear decoupled ¹H NMR spectra were recorded on a Bruker Advance 500 MHz spectrometer at 300 K. The ¹H NMR spectra were referenced internally to the residual proton impurity peaks according to the literature.³⁷ Elemental analysis data (C, H, and N) were obtained using a Thermo Scientific™ FLASH™ 2000 Organic Elemental Analyzer. Gel permeation chromatography (GPC) measurements were conducted on a Polymer Laboratories PL-GPC-220 instrument equipped with PLgel 5 μ m MIXED-D 300 \times 7.5 mm columns, and tetrahydrofuran (THF) was used as the eluent (flow rate: 1 mL min⁻¹ at 40 °C). The number-average molecular weights (M_n) and polydispersity indices (M_w/M_n) were calibrated against polystyrene (PS) standards.

General protocol for the synthesis of ligands HL¹–HL⁹

The reaction was performed according to the procedure previously reported in the literature, and the synthesis of compounds 1–9 is described in the ESI.†²⁵ The following example is typical. To a stirred solution of 1 (56.28 mmol) in dichloromethane (100 mL), 2,3-dichloro-5,6-dicyano-1,4-benzoquinone (67.53 mmol) was added. The reaction mixture was stirred at room temperature for 15 h. After removal of the volatiles, the dark color residue was purified by column chromatography (CH₂Cl₂ : hexane = 60 : 40). The desired ligands were obtained as white solids.

2-(2'-Hydroxyphenyl)benzoxazole (HL¹). Yield: 5.10 g, 45%. ¹H NMR (500.13 MHz, CDCl₃, 300 K): δ 11.47 (s, 1H, OH), 8.03 (dd, ⁴J_{HH} = 1.7 Hz, ³J_{HH} = 7.9 Hz, 1H, ArH), 7.74–7.72 (m, 1H, ArH), 7.62–7.60 (m, 1H, ArH), 7.46–7.42 (m, 1H, ArH), 7.40–7.37 (m, 2H, ArH), 7.14–7.12 (m, 1H, ArH), 7.03–6.99 (m, 1H, ArH). ¹³C NMR (125.77 MHz, CDCl₃, 300 K): δ 163.1 (C=N), 159.0 (ArC), 149.3 (ArC), 140.2 (ArC), 133.8 (ArCH), 127.3 (ArCH), 125.6 (ArCH), 125.2 (ArCH), 119.8 (ArCH), 119.4 (ArCH), 117.6 (ArCH), 110.9 (ArCH), 110.8 (ArC). Anal. calcd for C₁₃H₉NO₂: C 73.92, H 4.29, N 6.63; found: C 73.92, H 4.26, N 6.59.

2-(2'-Hydroxy-3',5'-dimethylphenyl)benzoxazole (HL²). Yield: 0.86 g, 11%. ¹H NMR (500.13 MHz, CDCl₃, 300 K): δ 11.46 (s, 1H, OH), 7.72–7.70 (m, 1H, ArH), 7.68 (s, 1H, ArH), 7.60–7.58 (m, 1H, ArH), 7.38–7.35 (m, 2H, ArH), 7.13 (s, 1H, ArH), 2.34 (s, 3H, CH₃), 2.33 (s, 3H, CH₃). ¹³C NMR (125.77 MHz, CDCl₃, 300 K): δ 163.7 (C=N), 155.2 (ArC), 149.4 (ArC), 140.4 (ArC), 135.9 (ArCH), 128.3 (ArC), 126.5 (ArC), 125.4 (ArCH), 125.1 (ArCH), 124.7 (ArCH), 119.4 (ArCH), 110.8 (ArCH), 109.6 (ArC), 20.7 (CH₃), 16.2 (CH₃). Anal. calcd for C₁₅H₁₃NO₂: C 75.30, H 5.48, N 5.85; found: C 75.27, H 5.55, N 5.88.

2-(2'-Hydroxy-3',5'-di-*tert*-butylphenyl)benzoxazole (HL³). Yield: 1.50 g, 75%. ¹H NMR data (500.13 MHz, CDCl₃, 300 K): δ 11.90 (br s, 1H, OH), 7.93 (d, ⁴J_{HH} = 2.5 Hz, 1H, ArH), 7.72–7.70 (m, 1H, ArH), 7.64–7.61 (m, 1H, ArH), 7.52 (d, ⁴J_{HH} = 2.5 Hz, 1H, ArH), 7.38–7.36 (m, 2H, ArH), 1.51 (s, 9H, C(CH₃)₃), 1.40 (s, 9H, C(CH₃)₃). ¹³C NMR data (125.77 MHz, CDCl₃, 300 K): δ 164.3 (C=N), 156.1 (ArC), 149.3 (ArC), 141.4 (ArC), 140.3 (ArC), 137.5 (ArC), 128.7 (ArCH), 125.3 (ArCH), 125.1 (ArCH), 121.5 (ArCH), 119.2 (ArCH), 110.8 (ArCH), 110.0 (ArC), 35.6 (C(CH₃)₃), 34.7 (C(CH₃)₃), 31.8 (C(CH₃)₃), 29.8 (C(CH₃)₃). Anal. calcd for C₂₁H₂₅NO₂: C 77.98, H 7.79, N 4.33; found: C 77.89, H 7.78, N 4.30.

2-(2'-Hydroxy-3',5'-dichlorophenyl)benzoxazole (HL⁴). Yield: 0.50 g, 25%. ¹H NMR (500.13 MHz, CDCl₃, 300 K): δ 12.09 (s, 1H, OH), 7.92 (d, ⁴J_{HH} = 2.5 Hz, 1H, ArH), 7.77–7.74 (m, 1H, ArH), 7.64–7.61 (m, 1H, ArH), 7.50 (d, ⁴J_{HH} = 2.5 Hz, 1H, ArH), 7.44–7.42 (m, 2H, ArH). ¹³C NMR (125.77 MHz, CDCl₃, 300 K): δ 161.3 (C=N), 153.5 (ArC), 149.4 (ArC), 139.6 (ArC), 133.4 (ArCH), 126.5 (ArCH), 125.7 (ArCH), 125.1 (ArCH), 124.5 (ArC), 123.4 (ArC), 119.8 (ArCH), 112.5 (ArC), 111.1 (ArCH). Anal. calcd for C₁₃H₇Cl₂NO₂: C 55.74, H 2.52, N 5.00; found: C 55.74, H 2.33, N 4.94.

2-(2'-Hydroxy-3',5'-dibromophenyl)benzoxazole (HL⁵). Yield: 2.78 g, 59%. ¹H NMR (500.13 MHz, CDCl₃, 300 K): δ 12.21 (s, 1H, OH), 8.09 (d, ⁴J_{HH} = 2.4 Hz, 1H, ArH), 7.78 (d, ⁴J_{HH} = 2.4 Hz, 1H, ArH), 7.75–7.73 (m, 1H, ArH), 7.63–7.61 (m, 1H, ArH), 7.44–7.41 (m, 2H, ArH). ¹³C NMR (125.77 MHz, CDCl₃, 300 K): δ 161.0 (C=N), 154.7 (ArC), 149.5 (ArC), 139.6 (ArC), 138.9 (ArCH), 128.8 (ArCH), 126.5 (ArCH), 125.7 (ArCH), 119.8 (ArCH), 112.9 (ArC), 112.5 (ArC), 111.4 (ArC), 111.1 (ArCH). Anal. calcd for C₁₃H₇Br₂NO₂: C 42.31, H 1.91, N 3.80; found: C 42.11, H 1.60, N 3.61.

2-(2'-Hydroxy-3'-isopropylphenyl)benzoxazole (HL⁶). Yield: 4.72 g, 74%. ¹H NMR (500.13 MHz, CDCl₃, 300 K): δ 11.76 (s, 1H, OH), 7.90 (dd, ⁴J_{HH} = 1.6 Hz, ³J_{HH} = 7.8 Hz, 1H, ArH), 7.73–7.71 (m, 1H, ArH), 7.62–7.59 (m, 1H, ArH), 7.40–7.36 (m, 3H, ArH), 6.98 (t, ³J_{HH} = 7.9 Hz, 1H, ArH), 3.50 (sept, 1H, CH(CH₃)₂), 1.32 (d, ³J_{HH} = 6.9 Hz, 6H, CH(CH₃)₂). ¹³C NMR (125.77 MHz, CDCl₃, 300 K): δ 163.7 (C=N), 156.6 (ArC), 149.4 (ArC), 140.3 (ArC), 137.0 (ArC), 130.4 (ArCH), 125.4 (ArCH), 125.1 (ArCH), 124.8 (ArCH), 119.5 (ArCH), 119.4 (ArCH), 110.8 (ArCH), 110.2 (ArC), 27.2 (CH(CH₃)₂), 22.6 (CH(CH₃)₂). Anal. calcd for C₁₆H₁₅NO₂: C 75.87, H 5.97, N 5.53; found: C 75.98, H 6.00, N 5.53.

2-(2'-Hydroxy-3'-*tert*-butylphenyl)benzoxazole (HL⁷). Yield: 3.80 g, 38%. ¹H NMR (500.13 MHz, CDCl₃, 300 K): δ 12.07 (br s, 1H, OH), 7.94 (d, ³J_{HH} = 7.8 Hz, 1H, ArH), 7.73–7.71 (m, 1H, ArH), 7.61–7.60 (m, 1H, ArH), 7.47 (d, ³J_{HH} = 7.7 Hz, 1H, ArH), 7.38–7.37 (m, 2H, ArH), 6.95 (t, ³J_{HH} = 7.7 Hz, 1H, ArH), 1.51 (s, 9H, C(CH₃)₃). ¹³C NMR (125.77 MHz, CDCl₃, 300 K): δ 163.9 (C=N), 158.2 (ArC), 149.3 (ArC), 140.2 (ArC), 138.1 (ArC), 131.0 (ArCH), 125.4 (ArCH), 125.1 (ArCH), 119.3 (ArCH), 119.1 (ArCH), 110.9 (ArC), 110.8 (ArCH), 35.3 (C(CH₃)₃), 29.6 (C(CH₃)₃). Anal. calcd for C₁₇H₁₇NO₂: C 76.38, H 6.41, N 5.24; found: C 76.25, H 6.10, N 5.14.

2-(2'-Hydroxy-3'-phenylphenyl)benzoxazole (HL⁸). Yield: 3.90 g, 78%. ¹H NMR (500.13 MHz, CDCl₃, 300 K): δ 8.06 (dd,

$^4J_{\text{HH}} = 1.7$ Hz, $^3J_{\text{HH}} = 7.9$ Hz, 1H, ArH), 7.73–7.69 (m, 3H, ArH), 7.64–7.62 (m, 1H, ArH), 7.54–7.47 (m, 3H, ArH), 7.42–7.38 (m, 3H, ArH), 7.10 (t, $^3J_{\text{HH}} = 7.7$ Hz, 1H, ArH), 4.91 (br s, 1H, OH). ^{13}C NMR (125.77 MHz, CDCl_3 , 300 K): δ 163.4 (C=N), 156.3 (ArC), 149.4 (ArC), 140.1 (ArC), 137.9 (ArC), 134.8 (ArCH), 130.6 (ArC), 129.8 (ArCH), 128.5 (ArCH), 127.6 (ArCH), 126.7 (ArCH), 125.7 (ArCH), 125.3 (ArCH), 119.8 (ArCH), 119.5 (ArCH), 111.1 (ArC), 110.9 (ArCH). Anal. calcd for $\text{C}_{19}\text{H}_{13}\text{NO}_2$: C 79.43, H 4.56, N 4.88; found: C 79.41, H 4.49, N 4.82.

2-(2'-Hydroxy-3'-(1,1-diphenylethyl)-5'-methylphenyl)benzoxazole (HL⁹). Yield: 1.02 g, 20%. ^1H NMR data (500.13 MHz, CDCl_3 , 300 K): δ 11.78 (s, 1H, OH), 7.81–7.80 (m, 1H, ArH), 7.61–7.58 (m, 2H, ArH), 7.36–7.33 (m, 2H, ArH), 7.32–7.30 (m, 4H, ArH), 7.26–7.21 (m, 6H, ArH), 6.67 (d, $^4J_{\text{HH}} = 2.1$ Hz, 1H, ArH), 2.42 (s, 3H, CH_3), 2.24 (s, 3H, CH_3). ^{13}C NMR data (125.77 MHz, CDCl_3 , 300 K): δ 163.6 (C=N), 155.7 (ArC), 149.4 (ArC), 148.5 (ArC), 140.2 (ArC), 136.9 (ArC), 135.7 (ArCH), 128.7 (ArCH), 128.1 (ArCH), 127.8 (ArC), 126.1 (ArCH), 126.0 (ArCH), 125.5 (ArCH), 125.2 (ArCH), 119.3 (ArCH), 110.8 (ArC), 110.7 (ArCH), 52.2 (C), 28.0 (CH_3), 21.1 (CH_3). Anal. calcd for $\text{C}_{28}\text{H}_{23}\text{NO}_2$: C 82.94, H 5.72, N 3.45; found: C 82.93, H 5.73, N 3.32.

General protocol for the synthesis of aluminum complexes 1a–9a

In a typical procedure, to a stirred solution of **HL**¹ (4.73 mmol) in toluene (30 mL) trimethylaluminum (TMA) (2.37 mL of a 2.0 M solution in toluene, 4.73 mmol) was slowly added at room temperature. The reaction mixture was stirred at room temperature for 24 h. The volatiles were removed under reduced pressure to leave a pale yellow solid, which was then recrystallized in hexane at -20 °C. The desired complexes were obtained as off-white solids.

L¹AlMe₂ (1a). Yield: 0.65 g, 52%. ^1H NMR (500.13 MHz, CDCl_3 , 300 K): δ 7.99 (dd, $^4J_{\text{HH}} = 1.8$ Hz, $^3J_{\text{HH}} = 8.0$ Hz, 1H, ArH), 7.69–7.67 (m, 2H, ArH), 7.51–7.46 (m, 3H, ArH), 7.02–7.00 (m, 1H, ArH), 6.89–6.85 (m, 1H, ArH), -0.60 (s, 6H, $\text{Al}(\text{CH}_3)_2$). ^{13}C NMR (125.77 MHz, CDCl_3 , 300 K): δ 165.6 (C=N), 164.4 (ArC), 148.8 (ArC), 136.9 (ArCH), 135.4 (ArC), 128.2 (ArCH), 126.8 (ArCH), 126.6 (ArCH), 122.5 (ArCH), 118.0 (ArCH), 116.9 (ArCH), 111.6 (ArCH), 109.8 (ArC), -9.2 ($\text{Al}(\text{CH}_3)_2$). Anal. calcd for $\text{C}_{15}\text{H}_{14}\text{AlNO}_2$: C 67.41, H 5.28, N 5.24; found: C 67.34, H 5.41, N 5.23.

L²AlMe₂ (2a). Yield: 0.78 g, 63%. ^1H NMR (500.13 MHz, CDCl_3 , 300 K): δ 7.67–7.64 (m, 2H, ArH), 7.63 (s, 1H, ArH), 7.47–7.44 (m, 2H, ArH), 7.22 (s, 1H, ArH), 2.31 (s, 3H, CH_3), 2.27 (s, 3H, CH_3), -0.60 (s, 6H, $\text{Al}(\text{CH}_3)_2$). ^{13}C NMR (125.77 MHz, CDCl_3 , 300 K): δ 166.2 (C=N), 161.4 (ArC), 148.8 (ArC), 138.7 (ArCH), 135.6 (ArC), 130.8 (ArC), 126.4 (ArCH), 124.9 (ArCH), 116.8 (ArCH), 111.4 (ArCH), 108.3 (ArC), 20.6 (CH_3), 16.7 (CH_3), -9.2 ($\text{Al}(\text{CH}_3)_2$). Anal. calcd for $\text{C}_{17}\text{H}_{18}\text{AlNO}_2$: C 69.14, H 6.14, N 4.74; found: C 69.08, H 6.12, N 4.58.

L³AlMe₂ (3a). Yield: 0.48 g, 41%. ^1H NMR (500.13 MHz, CDCl_3 , 300 K): δ 7.86 (d, $^4J_{\text{HH}} = 2.6$ Hz, 1H, ArH), 7.70–7.64 (m, 2H, ArH), 7.60 (d, $^4J_{\text{HH}} = 2.6$ Hz, 1H, ArH), 7.48–7.45

(m, 2H, ArH), 1.47 (s, 9H, $\text{C}(\text{CH}_3)_3$), 1.38 (s, 9H, $\text{C}(\text{CH}_3)_3$), -0.62 (s, 6H, $\text{Al}(\text{CH}_3)_2$). ^{13}C NMR (125.77 MHz, CDCl_3 , 300 K): δ 166.8 (C=N), 161.9 (ArC), 148.7 (ArC), 141.1 (ArC), 139.6 (ArC), 135.7 (ArC), 131.8 (ArCH), 126.4 (ArCH), 126.3 (ArCH), 121.8 (ArCH), 116.7 (ArCH), 111.4 (ArCH), 109.2 (ArC), 35.7 ($\text{C}(\text{CH}_3)_3$), 34.6 ($\text{C}(\text{CH}_3)_3$), 31.6 ($\text{C}(\text{CH}_3)_3$), 29.6 ($\text{C}(\text{CH}_3)_3$), -9.7 ($\text{Al}(\text{CH}_3)_2$). Anal. calcd for $\text{C}_{23}\text{H}_{30}\text{AlNO}_2$: C 72.80, H 7.97, N 3.69; found: C 72.56, H 8.23, N 3.66.

L⁴AlMe₂ (4a). Yield: 0.65 g, 54%. ^1H NMR (500.13 MHz, CDCl_3 , 300 K): δ 7.89 (d, $^4J_{\text{HH}} = 2.7$ Hz, 1H, ArH), 7.73–7.70 (m, 2H, ArH), 7.58 (d, $^4J_{\text{HH}} = 2.7$ Hz, 1H, ArH), 7.56–7.53 (m, 2H, ArH), -0.57 (s, 6H, $\text{Al}(\text{CH}_3)_2$). ^{13}C NMR (125.77 MHz, CDCl_3 , 300 K): δ 163.8 (C=N), 158.4 (ArC), 148.9 (ArC), 136.0 (ArCH), 135.1 (ArC), 127.8 (ArC), 127.6 (ArCH), 127.2 (ArCH), 125.6 (ArCH), 122.0 (ArC), 117.3 (ArCH), 111.8 (ArCH), 111.2 (ArC), -9.6 ($\text{Al}(\text{CH}_3)_2$). Anal. calcd for $\text{C}_{15}\text{H}_{12}\text{AlCl}_2\text{NO}_2$: C 53.60, H 3.60, N 4.17; found: C 53.50, H 3.57, N 3.97.

L⁵AlMe₂ (5a). Yield: 0.48 g, 42%. ^1H NMR (500.13 MHz, CDCl_3 , 300 K): δ 8.08 (d, $^4J_{\text{HH}} = 2.5$ Hz, 1H, ArH), 7.88 (d, $^4J_{\text{HH}} = 2.5$ Hz, 1H, ArH), 7.73–7.70 (m, 2H, ArH), 7.56–7.53 (m, 2H, ArH), -0.58 (s, 6H, $\text{Al}(\text{CH}_3)_2$). ^{13}C NMR (125.77 MHz, CDCl_3 , 300 K): δ 163.6 (C=N), 159.4 (ArC), 148.9 (ArC), 141.5 (ArCH), 135.1 (ArC), 129.4 (ArCH), 127.6 (ArCH), 127.2 (ArCH), 118.0 (ArC), 117.2 (ArCH), 111.8 (ArCH), 111.6 (ArC), 108.8 (ArC) -9.6 ($\text{Al}(\text{CH}_3)_2$). Anal. calcd for $\text{C}_{15}\text{H}_{12}\text{AlBr}_2\text{NO}_2$: C 42.39, H 2.80, N 3.30; found: C 42.70, H 3.08, N 3.70.

L⁶AlMe₂ (6a). Yield: 0.74 g, 61%. ^1H NMR (500.13 MHz, CDCl_3 , 300 K): δ 7.85 (d, $^3J_{\text{HH}} = 8.0$ Hz, 1H, ArH), 7.68–7.66 (m, 2H, ArH), 7.48–7.46 (m, 2H, ArH), 7.43 (d, $^3J_{\text{HH}} = 7.3$ Hz, 1H, ArH), 6.85 (t, $^3J_{\text{HH}} = 7.7$ Hz, 1H, ArH), 3.49 (sept, 1H, $\text{CH}(\text{CH}_3)_2$), 1.26 (d, $^3J_{\text{HH}} = 6.9$ Hz, 6H, $\text{CH}(\text{CH}_3)_2$), -0.60 (s, 6H, $\text{Al}(\text{CH}_3)_2$). ^{13}C NMR (125.77 MHz, CDCl_3 , 300 K): δ 166.2 (C=N), 162.3 (ArC), 148.8 (ArC), 141.1 (ArC), 135.6 (ArC), 132.8 (ArCH), 126.5 (ArCH), 125.5 (ArCH), 117.6 (ArCH), 116.8 (ArCH), 111.4 (ArCH), 109.2 (ArC), 27.3 ($\text{CH}(\text{CH}_3)_2$), 22.4 ($\text{CH}(\text{CH}_3)_2$), -9.6 ($\text{Al}(\text{CH}_3)_2$). Anal. calcd for $\text{C}_{18}\text{H}_{20}\text{AlNO}_2$: C 69.89, H 6.52, N 4.53; found: C 69.75, H 6.52, N 4.50.

L⁷AlMe₂ (7a). Yield: 0.65 g, 54%. ^1H NMR (500.13 MHz, CDCl_3 , 300 K): δ 7.92 (dd, $^4J_{\text{HH}} = 1.8$ Hz, $^3J_{\text{HH}} = 8.0$ Hz, 1H, ArH), 7.70–7.68 (m, 2H, ArH), 7.75 (dd, $^4J_{\text{HH}} = 1.8$ Hz, $^3J_{\text{HH}} = 7.7$ Hz, 1H, ArH), 7.51–7.49 (m, 2H, ArH), 6.84 (t, $^3J_{\text{HH}} = 7.9$ Hz, 1H, ArH), 1.48 (s, 9H, $\text{C}(\text{CH}_3)_3$), -0.57 (s, 6H, $\text{Al}(\text{CH}_3)_2$). ^{13}C NMR (125.77 MHz, CDCl_3 , 300 K): δ 166.4 (C=N), 163.7 (ArC), 148.7 (ArC), 141.8 (ArC), 135.6 (ArC), 123.6 (ArCH), 126.5 (ArCH), 126.4 (ArCH), 126.3 (ArCH), 117.4 (ArCH), 116.7 (ArCH), 111.4 (ArCH), 110.2 (ArC), 35.5 ($\text{C}(\text{CH}_3)_3$), 29.5 ($\text{C}(\text{CH}_3)_3$), -9.8 ($\text{Al}(\text{CH}_3)_2$). Anal. calcd for $\text{C}_{19}\text{H}_{22}\text{AlNO}_2$: C 70.57, H 6.86, N 4.33; found: C 70.67, H 6.86, N 4.23.

L⁸AlMe₂ (8a). Yield: 0.53 g, 44%. ^1H NMR (500.13 MHz, CDCl_3 , 300 K): δ 8.02 (dd, $^4J_{\text{HH}} = 1.8$ Hz, $^3J_{\text{HH}} = 8.0$ Hz, 1H, ArH), 7.70–7.67 (m, 4H, ArH), 7.60 (dd, $^4J_{\text{HH}} = 1.8$ Hz, $^3J_{\text{HH}} = 7.4$ Hz, 1H, ArH), 7.51–7.44 (m, 4H, ArH), 7.38–7.34 (m, 1H, ArH), 6.96 (t, $^3J_{\text{HH}} = 7.7$ Hz, 1H, ArH), -0.60 (s, 6H, $\text{Al}(\text{CH}_3)_2$). ^{13}C NMR (125.77 MHz, CDCl_3 , 300 K): δ 165.8 (C=N), 161.8 (ArC), 148.8 (ArC), 138.6 (ArC), 137.5 (ArCH), 135.5 (ArC), 134.1 (ArC), 129.7 (ArCH), 128.2 (ArCH), 127.6 (ArCH), 127.2 (ArCH),

126.8 (ArCH), 126.6 (ArCH), 118.0 (ArCH), 117.0 (ArCH), 111.5 (ArCH), 110.5 (ArC), -9.4 (Al(CH₃)₂). Anal. calcd for C₂₁H₁₈AlNO₂: C 73.46, H 5.28, N 4.08; found: C 73.46, H 5.25, N 4.02.

L⁹AlMe₂ (9a). Yield: 0.71 g, 62%. ¹H NMR (500.13 MHz, CDCl₃, 300 K): δ 7.76 (m, 1H, ArH), 7.67–7.65 (m, 1H, ArH), 7.59–7.58 (m, 1H, ArH), 7.47–7.44 (m, 2H, ArH), 7.30–7.27 (m, 4H, ArH), 7.24–7.19 (m, 6H, ArH), 6.91 (m, 1H, ArH), 2.34 (s, 3H, CH₃), 2.25 (s, 3H, CH₃), -0.93 (s, 6H, Al(CH₃)₂). ¹³C NMR (125.77 MHz, CDCl₃, 300 K): δ 166.1 (C=N), 161.2 (ArC), 148.7 (ArC), 148.3 (ArCH), 140.8 (ArC), 138.7 (ArCH), 135.6 (ArC), 128.6 (ArCH), 127.9 (ArCH), 126.5 (ArC), 126.4 (ArCH), 126.3 (ArCH), 125.8 (ArC), 125.7 (ArCH), 116.7 (ArCH), 111.3 (ArCH), 109.9 (ArC), 52.1 (C), 28.2 (CH₃), 21.0 (CH₃), -10.1 (Al(CH₃)₂). Anal. calcd for C₃₀H₂₈AlNO₂: C 78.07, H 6.11, N 3.03; found: C 78.05, H 6.17, N 2.87.

General protocol for the synthesis of aluminum complexes 1b–9b

In a typical procedure, to a stirred solution of HL¹ (4.73 mmol) in toluene (30 mL), trimethylaluminum (1.18 mL of a 2.0 M solution in toluene, 2.36 mmol) was slowly added at room temperature. The reaction mixture was stirred at 100 °C for 15 h. After cooling to room temperature, a solid precipitated. The desired complexes were obtained as off-white solids.

L¹AlMe (1b). Yield: 0.62 g, 57%. ¹H NMR (500.13 MHz, CDCl₃, 300 K): δ 8.11–8.09 (m, 2H, ArH), 8.06–8.04 (m, 2H, ArH), 7.69–7.66 (m, 2H, ArH), 7.49–7.45 (m, 4H, ArH), 7.44–7.39 (m, 2H, ArH), 6.92–6.86 (m, 4H, ArH), -0.76 (s, 3H, AlCH₃). ¹³C NMR (125.77 MHz, CDCl₃, 300 K): δ 164.0 (C=N), 163.8 (ArC), 149.2 (ArC), 137.8 (ArC), 135.3 (ArCH), 127.6 (ArCH), 125.7 (ArCH), 125.6 (ArCH), 122.0 (ArCH), 119.7 (ArCH), 117.7 (ArCH), 111.2 (ArC), 110.9 (ArCH), 0.24 (AlCH₃). Anal. calcd for C₂₇H₁₉AlN₂O₄: C 70.13, H 4.14, N 6.06; found: C 70.26, H 4.10, N 6.01.

L²AlMe (2b). Yield: 0.56 g, 52%. ¹H NMR (500.13 MHz, CDCl₃, 300 K): δ 8.06–8.05 (m, 2H, ArH), 7.69 (s, 2H, ArH), 7.65–7.63 (m, 2H, ArH), 7.43–7.41 (m, 4H, ArH), 7.09 (s, 2H, ArH), 2.30 (s, 6H, CH₃), 1.86 (s, 6H, CH₃), -0.60 (s, 3H, AlCH₃). ¹³C NMR (125.77 MHz, CDCl₃, 300 K): δ 164.1 (C=N), 160.7 (ArC), 149.1 (ArC), 137.8 (ArC), 137.1 (ArCH), 130.4 (ArC), 125.8 (ArC), 125.5 (ArCH), 125.1 (ArCH), 124.4 (ArCH), 119.9 (ArCH), 110.6 (ArCH), 109.5 (ArC), 20.6 (CH₃), 17.0 (CH₃), -6.2 (AlCH₃). Anal. calcd for C₃₁H₂₇AlN₂O₄: C 71.80, H 5.25, N 5.40; found: C 71.83, H 5.27, N 5.39.

L³AlMe (3b). Yield: 0.45 g, 42%. ¹H NMR (500.13 MHz, CDCl₃, 300 K): δ 8.06–8.04 (m, 2H, ArH), 7.88 (d, ⁴J_{HH} = 2.6 Hz, 2H, ArH), 7.68–7.65 (m, 2H, ArH), 7.45–7.43 (m, 4H, ArH), 7.40 (d, ⁴J_{HH} = 2.6 Hz, 2H, ArH), 1.32 (s, 9H, C(CH₃)₃), 0.90 (s, 9H, C(CH₃)₃), -0.11 (s, 3H, AlCH₃). ¹³C NMR (125.77 MHz, CDCl₃, 300 K): δ 164.7 (C=N), 161.0 (ArC), 149.0 (ArC), 140.1 (ArC), 138.9 (ArC), 137.8 (ArC), 130.2 (ArCH), 125.4 (ArCH), 125.0 (ArCH), 121.6 (ArCH), 120.2 (ArCH), 110.5 (ArCH), 110.3 (ArC), 34.9 (C(CH₃)₃), 34.5 (C(CH₃)₃), 31.6 (C(CH₃)₃), 29.0 (C(CH₃)₃), -3.8 (AlCH₃). Anal. calcd for C₄₃H₅₁AlN₂O₄: C 75.19, H 7.48, N 4.08; found: C 75.51, H 7.73, N 4.43.

L⁴AlMe (4b). Yield: 0.60 g, 56%. ¹H NMR (500.13 MHz, toluene-*d*₈, 343 K): δ 8.23 (d, ³J_{HH} = 8.3 Hz, 2H, ArH), 7.62 (d, ⁴J_{HH} = 2.7 Hz, 2H, ArH), 7.29 (d, ⁴J_{HH} = 2.7 Hz, 2H, ArH), 7.23–7.16 (m, 4H, ArH), 7.08–7.06 (m, 2H, ArH), -0.20 (s, 3H, AlCH₃). ¹³C NMR (125.77 MHz, toluene-*d*₈, 343 K): δ 134.6 (ArCH), 126.6 (ArCH), 125.7 (ArCH), 125.6 (ArCH), 122.1 (ArC), 121.4 (ArCH), 110.7 (ArCH). It is noted that some signals in the ¹³C NMR spectrum could not be assigned because they were overlapped with the dominant toluene-*d*₈ peaks. Anal. calcd for C₂₇H₁₅AlCl₄N₂O₄: C 54.03, H 2.52, N 4.67; found: C 54.33, H 2.52, N 4.39.

L⁵AlMe (5b). Yield: 0.64 g, 61%. ¹H NMR (500.13 MHz, CDCl₃, 300 K): δ 8.14 (d, ⁴J_{HH} = 2.5 Hz, 2H, ArH), 8.13–8.12 (m, 2H, ArH), 7.75 (d, ⁴J_{HH} = 2.5 Hz, 2H, ArH), 7.68–7.66 (m, 4H, ArH), -0.56 (s, 3H, AlCH₃). ¹³C NMR (125.77 MHz, CDCl₃, 300 K): δ 161.3 (C=N), 149.1 (ArC), 140.5 (ArC), 139.9 (ArCH), 136.7 (ArC), 129.0 (ArCH), 126.6 (ArCH), 125.6 (ArCH), 121.3 (ArCH), 117.6 (ArC), 113.0 (ArC), 110.7 (ArCH), 108.6 (ArC). Anal. calcd for C₂₇H₁₅AlBr₄N₂O₄: C 41.68, H 1.94, N 3.60; found: C 41.88, H 1.96, N 3.60.

L⁶AlMe (6b). Yield: 0.55 g, 51%. ¹H NMR (500.13 MHz, CDCl₃, 300 K): δ 8.07–8.06 (m, 2H, ArH), 7.88 (d, ³J_{HH} = 8.0 Hz, 2H, ArH), 7.68–7.65 (m, 2H, ArH), 7.47–7.43 (m, 4H, ArH), 7.27 (d, ³J_{HH} = 7.9 Hz, 2H, ArH), 6.80 (t, ³J_{HH} = 7.7 Hz, 2H, ArH), 2.97 (sept, 2H, CH(CH₃)₂), 0.98 (d, ³J_{HH} = 6.9 Hz, 6H, CH(CH₃)₂), 0.60 (d, ³J_{HH} = 6.8 Hz, 6H, CH(CH₃)₂), -0.39 (s, 3H, AlCH₃). ¹³C NMR (125.77 MHz, CDCl₃, 300 K): δ 164.1 (C=N), 161.5 (ArC), 149.0 (ArC), 140.6 (ArC), 137.8 (ArC), 131.1 (ArCH), 125.6 (ArCH), 125.0 (ArCH), 124.9 (ArCH), 119.8 (ArCH), 117.1 (ArCH), 110.7 (ArCH), 110.1 (ArC), 26.2 (CH(CH₃)₂), 22.8 (CH(CH₃)₂), 22.2 (CH(CH₃)₂). Anal. calcd for C₃₃H₃₁AlN₂O₄: C 72.51, H 5.72, N 5.13; found: C 72.55, H 5.73, N 5.13.

L⁷AlMe (7b). Yield: 0.59 g, 55%. ¹H NMR (500.13 MHz, CDCl₃, 300 K): δ 8.06–8.04 (m, 2H, ArH), 7.92 (dd, ⁴J_{HH} = 1.8 Hz, ³J_{HH} = 8.0 Hz, 2H, ArH), 7.66–7.64 (m, 2H, ArH), 7.46–7.44 (m, 4H, ArH), 7.33 (dd, ⁴J_{HH} = 1.8 Hz, ³J_{HH} = 7.5 Hz, 2H, ArH), 6.74 (t, ³J_{HH} = 7.8 Hz, 2H, ArH), 0.88 (s, 18H, C(CH₃)₃), -0.08 (s, 3H, AlCH₃). ¹³C NMR (125.77 MHz, CDCl₃, 300 K): δ 164.4 (C=N), 162.8 (ArC), 149.0 (ArC), 140.9 (ArC), 137.6 (ArC), 132.1 (ArCH), 126.0 (ArCH), 125.6 (ArCH), 123.1 (ArCH), 120.2 (ArCH), 116.9 (ArCH), 111.3 (ArC), 110.6 (ArCH), 34.6 (C(CH₃)₃), 28.9 (C(CH₃)₃). Anal. calcd for C₃₅H₃₅AlN₂O₄: C 73.15, H 6.14, N 4.87; found: C 73.20, H 6.47, N 4.78.

L⁸AlMe (8b). Yield: 0.56 g, 52%. ¹H NMR (500.13 MHz, CDCl₃, 300 K): δ 8.10 (dd, ⁴J_{HH} = 1.8 Hz, ³J_{HH} = 7.9 Hz, 2H, ArH), 7.58 (td, ⁴J_{HH} = 0.9 Hz, ³J_{HH} = 7.1 Hz, 2H, ArH), 7.48 (dd, ⁴J_{HH} = 1.9 Hz, ³J_{HH} = 7.3 Hz, 2H, ArH), 7.29–7.25 (m, 8H, ArH), 6.96 (t, ⁴J_{HH} = 3.7 Hz, 2H, ArH), 6.87 (td, ⁴J_{HH} = 1.0 Hz, ³J_{HH} = 7.8 Hz, 2H, ArH), 6.74–6.65 (m, 6H, ArH), -0.73 (s, 3H, AlCH₃). ¹³C NMR (125.77 MHz, CDCl₃, 300 K): δ 163.3 (C=N), 161.2 (ArC), 148.6 (ArC), 138.6 (ArC), 137.5 (ArC), 135.8 (ArCH), 134.2 (ArC), 129.3 (ArCH), 127.0 (ArCH), 126.9 (ArCH), 126.6 (ArCH), 125.3 (ArCH), 125.1 (ArCH), 119.5 (ArCH), 117.5 (ArCH), 111.5 (ArC), 110.0 (ArCH), -6.0 (AlCH₃). Anal. calcd for C₃₉H₂₇AlN₂O₄: C 76.21, H 4.43, N 4.56; found: C 76.12, H 4.25, N 4.20.

L₂AlMe (9b). Yield: 0.42 g, 40%. ¹H NMR (500.13 MHz, CDCl₃, 300 K): δ 7.68–7.66 (m, 4H, ArH), 7.56–7.55 (m, 2H, ArH), 7.36 (td, ⁴J_{HH} = 1.1 Hz, ³J_{HH} = 7.4 Hz, 2H, ArH), 7.31–7.28 (m, 2H, ArH), 7.16–7.13 (m, 4H, ArH), 7.09–7.06 (m, 2H, ArH), 6.90 (d, ³J_{HH} = 7.6, 4H, ArH), 6.74 (d, ³J_{HH} = 7.0, 2H, ArH), 6.61 (t, ³J_{HH} = 7.1, 4H, ArH), 6.51 (d, ³J_{HH} = 7.6, 4H, ArH), 6.40 (s, 2H, ArH), 2.20 (s, 6H, CH₃), 1.98 (s, 6H, CH₃), –0.57 (s, 3H, AlCH₃). ¹³C NMR (125.77 MHz, CDCl₃, 300 K): δ 163.3 (C=N), 160.0 (ArC), 149.5 (ArC), 148.7 (ArC), 147.4 (ArC), 139.7 (ArC), 137.4 (ArC), 137.0 (ArCH), 128.9 (ArCH), 127.9 (ArCH), 127.0 (ArCH), 126.7 (ArCH), 126.8 (ArC), 125.7 (ArCH), 125.2 (ArCH), 125.1 (ArCH), 124.8 (ArCH), 124.4 (ArCH), 120.1 (ArCH), 111.6 (ArC), 110.3 (ArCH), 51.8 (C), 26.1 (CH₃), 21.2 (CH₃), –3.7 (AlCH₃). Anal. calcd for C₅₇H₄₇AlN₂O₄: C 80.45, H 5.57, N 3.29; found: C 80.47, H 5.61, N 3.29.

General polymerization procedure for *rac*-LA

In a nitrogen-filled glove box, *rac*-lactide (720 mg, 5.0 mmol) and benzyl alcohol (5.17 μL, 0.05 mmol) were placed in a polymerization ampoule. To this ampoule, a solution of the initiator (0.05 mmol) in toluene (6.00 mL) ([monomer]:[Al] = 100:1) was added. The reaction was stirred for the desired reaction time at 70 °C. Subsequently, the reaction was quenched with methanol (2–3 drops). The polymer was precipitated from excess methanol, collected by filtration and dried *in vacuo* to a constant mass. Conversions were determined by integration of the monomer *versus* polymer methine resonances in the ¹H NMR spectrum of the crude product (in CDCl₃).

General polymerization procedure for ε-CL

In a nitrogen-filled glove box, ε-caprolactone (570 mg, 5.0 mmol) and benzyl alcohol (5.17 μL, 0.05 mmol) were placed in a polymerization ampoule. To this ampoule a solution of the initiator (0.05 mmol) in toluene (3.00 mL) ([monomer]:[Al] = 100:1) was added. The reaction was stirred for the desired reaction time at 70 °C. At the desired reaction time, the reaction was quenched with methanol (2–3 drops). The polymer was precipitated from excess methanol, collected by filtration and dried *in vacuo* to a constant mass. Conversions were determined by integration of the monomer *versus* polymer methine resonances in the ¹H NMR spectrum of the crude product (in CDCl₃).

General procedure for kinetic studies

The polymerizations were carried out at 70 °C (for *rac*-LA) or 40 °C (for ε-CL) in a glove box. The molar ratio of monomer to initiator was fixed at 50:1. At appropriate time intervals, 0.5 μL aliquots were removed and quenched with methanol. The solvent was removed *in vacuo* and the percent conversion was determined by ¹H NMR in CDCl₃.

Crystal structure determination

X-ray diffraction data were collected on a Bruker APEX-II CCD diffractometer with graphite monochromated Mo Kα radiation (λ = 0.71073 Å) at 100 K. The structure of C₁₉H₂₂AlNO₂ (7a) was

solved by direct methods with SIR2004³⁸ and refined with Olex2.refine.³⁹ The structure of C₃₄H₂₇AlN₂O₄ (1b) was solved by XT⁴⁰ and refined with XL.⁴¹ Olex2⁴² is used for molecular graphic. Crystallographic data have been deposited at the Cambridge Crystallographic Data Centre under reference numbers CCDC 1429409 (1b) and 1429410 (7a).

Acknowledgements

We gratefully acknowledge financial support from Kasetsart University Research and Development Institute (KURDI) (grant no. 26.58), the National Research Council of Thailand (NRCT) and the Faculty of Science, Kasetsart University (grant no. ScRF-S21-2558). This research is also supported in part by the Graduate Program Scholarship from the Graduate School, Kasetsart University (P.T.). P. H. and P. C. thank Kasetsart University and the Center of Excellence for Innovation in Chemistry (PERCH-CIC), the Office of the Higher Education Commission, Ministry of Education for financial support. We also gratefully acknowledge Dr Kittiponk Chainok for his useful discussion on X-ray structure determination.

References

- (a) A. C. Albertsson and I. K. Varma, *Biomacromolecules*, 2003, **4**, 1466–1486; (b) R. E. Drumright, P. R. Gruber and D. E. Henton, *Adv. Mater.*, 2000, **12**, 1841–1846; (c) E. Chiellini and R. Solaro, *Adv. Mater.*, 1996, **8**, 305–313; (d) H. Winet and J. Y. Bao, *J. Biomed. Mater. Res.*, 1998, **40**, 567–576; (e) R. Gref, Y. Minamitake, M. T. Peracchia, V. Trubetskov, V. Torchilin and R. Langer, *Science*, 1994, **263**, 1600–1603.
- (a) B. J. O'Keefe, M. A. Hillmyer and W. B. Tolman, *J. Chem. Soc., Dalton Trans.*, 2001, 2215–2224; (b) O. Dechy-Cabaret, B. Martin-Vaca and D. Bourissou, *Chem. Rev.*, 2004, **104**, 6147–6176; (c) J. Wu, T.-L. Yu, C.-T. Chen and C.-C. Lin, *Coord. Chem. Rev.*, 2006, **250**, 602–626.
- (a) G. Li, M. Lamberti, D. Pappalardo and C. Pellicchia, *Macromolecules*, 2012, **45**, 8614–8620; (b) C. Bakewell, R. H. Platel, S. K. Cary, S. M. Hubbard, J. M. Roaf, A. C. Levine, A. J. P. White, N. J. Long, M. Haaf and C. K. Williams, *Organometallics*, 2012, **31**, 4729–4736; (c) M. Lamberti, I. D'Auria, M. Mazzeo, S. Milione, V. Bertolasi and D. Pappalardo, *Organometallics*, 2012, **31**, 5551–5560; (d) D. J. Darensbourg, O. Karroonnirun and S. J. Wilson, *Inorg. Chem.*, 2011, **50**, 6775–6787; (e) M. Normand, V. Dorcet, E. Kirillov and J.-F. Carpentier, *Organometallics*, 2013, **32**, 1694–1709; (f) N. Maudoux, T. Roisnel, V. Dorver, J.-F. Carpentier and Y. Sarazin, *Chem. – Eur. J.*, 2014, **20**, 6131–6147; (g) S. Tabthong, T. Nanok, P. Sumrit, P. Kongsaree, S. Prabpai, P. Chuawong and P. Hormnirun, *Macromolecules*, 2015, **48**, 6846–6861.
- (a) T. M. Ovitt and G. W. Coates, *J. Am. Chem. Soc.*, 1999, **121**, 4072–4073; (b) P. L. Arnold, J.-C. Buffet, R. Blaudeck,

- S. Sujecki and C. Wilson, *Chem. – Eur. J.*, 2009, **15**, 8241–8250; (c) A. Alaeddine, C. M. Thomas, T. Roisnel and J.-F. Carpentier, *Organometallics*, 2009, **28**, 1469–1475; (d) J.-C. Buffet, A. Kapelski and J. Okuda, *Macromolecules*, 2010, **43**, 10201–10203; (e) R. H. Platel, A. J. P. White and C. K. Williams, *Inorg. Chem.*, 2011, **50**, 7718–7728; (f) T.-P.-A. Cao, A. Buchard, X. F. Le Goff, A. Auffrant and C. K. Williams, *Inorg. Chem.*, 2012, **51**, 2157–2169; (g) S. Yang, Z. Du, Y. Zhang and Q. Shen, *Chem. Commun.*, 2012, **48**, 9780–9782; (h) C. Bakewell, A. J. P. White, N. J. Long and C. K. Williams, *Inorg. Chem.*, 2015, **54**, 2204–2212.
- 5 (a) P. Horeglad, P. Kruk and J. Pécaut, *Organometallics*, 2010, **29**, 3729–3734; (b) P. Horeglad, G. Szczepaniak, M. Dranka and J. Zachara, *Chem. Commun.*, 2012, **48**, 1171–1173; (c) C. Bakewell, A. J. P. White, N. J. Long and C. K. Williams, *Inorg. Chem.*, 2013, **52**, 12561–12567; (d) P. Horeglad, O. Ablialimov, G. Szczepaniak, A. M. Dabrowska, M. Dranka and J. Zachara, *Organometallics*, 2014, **33**, 100–111.
- 6 (a) I. D'Auria, M. Lamberti, M. Mazzeo, S. Milione, G. Roviello and C. Pellicchia, *Chem. – Eur. J.*, 2012, **18**, 2349–2360; (b) F. Drouin, P. O. Oguadinma, T. J. J. Whitehorne, R. E. Prud'homme and F. Schaper, *Organometallics*, 2010, **29**, 2139–2147; (c) H. Wang, Y. Yang and H. Ma, *Macromolecules*, 2014, **47**, 7750–7764.
- 7 (a) A. P. Dove, V. C. Gibson, E. L. Marshall, A. J. P. White and D. J. Williams, *Chem. Commun.*, 2001, 283–284; (b) K. B. Aubrecht, M. A. Hillmyer and W. B. Tolman, *Macromolecules*, 2002, **35**, 644–650.
- 8 (a) Y. Kim, G. K. Jnaneshwara and J. G. Verkade, *Inorg. Chem.*, 2003, **42**, 1437–1447; (b) S. Gendler, S. Segal, I. Goldberg, Z. Goldschmidt and M. Kol, *Inorg. Chem.*, 2006, **45**, 4783–4790; (c) C. J. Chuck, M. G. Davidson, M. D. Jones, G. Kociok-Köhn, M. D. Lunn and S. Wu, *Inorg. Chem.*, 2006, **45**, 6595–6597; (d) S. H. Kim, J. Lee, D. J. Kim, J. H. Moon, S. Yoon, H. J. Oh, Y. Do, Y. S. Ko, J.-H. Yim and Y. Kim, *J. Organomet. Chem.*, 2009, **694**, 3409–3417; (e) C.-Y. Li, C.-J. Yu and B.-T. Ko, *Organometallics*, 2013, **32**, 172–180; (f) C. Bakewell, G. Feteş-Iravani, D. W. Beh, D. Myers, S. Tabthong, P. Hormnirun, A. J. P. White, N. J. Long and C. K. Williams, *Dalton Trans.*, 2015, **44**, 12326–12337.
- 9 (a) H. Ma, T. P. Spaniol and J. Okuda, *Angew. Chem., Int. Ed.*, 2006, **118**, 7982–7985; (b) M. Sinenkov, E. Kirillov, T. Roisnel, G. Fukin, A. Trifonov and J.-F. Carpentier, *Organometallics*, 2011, **30**, 5509–5523; (c) A. Buchard, R. H. Platel, A. Auffrant, X. F. Le Goff, P. Le Floch and C. K. Williams, *Organometallics*, 2010, **29**, 2892–2900; (d) W. M. Stevels, M. J. K. Ankoné, P. J. Dijkstra and J. Feijen, *Macromolecules*, 1996, **29**, 3332–3333; (e) M. Zhang, X. Ni and Z. Shen, *Organometallics*, 2014, **33**, 6861–6867.
- 10 (a) R. H. Platel, L. M. Hodgson and C. K. Williams, *Polym. Rev.*, 2008, **48**, 11–63; (b) C. A. Wheaton, P. G. Hayes and B. J. Ireland, *Dalton Trans.*, 2009, 4832–4846; (c) A. P. Dove, *Chem. Commun.*, 2008, 6446–6470; (d) C. M. Thomas, *Chem. Soc. Rev.*, 2010, **39**, 165–173; (e) M. J. Stanford and A. P. Dove, *Chem. Soc. Rev.*, 2010, **39**, 486–494; (f) A. Arbaoui and C. Redshaw, *Polym. Chem.*, 2010, **1**, 801–826; (g) P. J. Dijkstra, H. Du and J. Feijen, *Polym. Chem.*, 2011, **2**, 520–527; (h) S. M. Guillaume, E. Kirillov, Y. Sarazin and J.-F. Carpentier, *Chem. – Eur. J.*, 2015, **21**, 7988–8003.
- 11 (a) M. Shen, W. Zhang, K. Nomura and W.-H. Sun, *Dalton Trans.*, 2009, 9000–9009; (b) T. Aida and S. Inoue, *Acc. Chem. Res.*, 1996, **29**, 39–48.
- 12 (a) N. Nomura, R. Ishii, M. Akakura and K. Aoi, *J. Am. Chem. Soc.*, 2002, **124**, 5938–5939; (b) Z. Tang, X. Chen, X. Pang, Y. Yang, X. Zhang and X. Jing, *Biomacromolecules*, 2004, **5**, 965–970; (c) P. Hormnirun, E. L. Marshall, V. C. Gibson, R. I. Pugh and A. J. P. White, *Proc. Natl. Acad. Sci. U. S. A.*, 2006, **103**, 15343–15348; (d) N. Nomura, R. Ishii, Y. Yamamoto and T. Kondo, *Chem. – Eur. J.*, 2007, **13**, 4433–4451; (e) H. Du, X. Pang, H. Yu, X. Zhuang, X. Chen, D. Cui, X. Wang and X. Jing, *Macromolecules*, 2007, **40**, 1904–1913; (f) M. H. Chisholm, J. C. Gallucci, K. T. Quisenberry and Z. Zhou, *Inorg. Chem.*, 2008, **47**, 2613–2624; (g) H.-L. Chen, S. Dutta, P.-Y. Huang and C.-C. Lin, *Organometallics*, 2012, **31**, 2016–2025; (h) E. D. Cross, L. E. N. Allan, A. Decken and M. P. Shaver, *J. Polym. Sci., Part A: Polym. Chem.*, 2013, **51**, 1137–1146; (i) C. Agatemor, A. E. Arnold, E. D. Cross, A. Decken and M. P. Shaver, *J. Organomet. Chem.*, 2013, **745–746**, 335–340; (j) E. E. Marlier, J. A. Macaranas, D. J. Marell, C. R. Dunbar, M. A. Johnson, Y. DePorre, M. O. Miranda, B. D. Neisen, C. J. Cramer, M. A. Hillmyer and W. B. Tolman, *ACS Catal.*, 2016, **6**, 1215–1224.
- 13 (a) P. Hormnirun, E. L. Marshall, V. C. Gibson, A. J. P. White and D. J. Williams, *J. Am. Chem. Soc.*, 2004, **126**, 2688–2689; (b) H. Du, A. H. Velders, P. J. Dijkstra, J. Sun, Z. Zhong, X. Chen and J. Feijen, *Chem. – Eur. J.*, 2009, **15**, 9836–9845; (c) Y. Wang and H. Ma, *Chem. Commun.*, 2012, **48**, 6729–6731; (d) P. Sumrit and P. Hormnirun, *Macromol. Chem. Phys.*, 2013, **214**, 1845–1851; (e) K. Press, I. Goldberg and M. Kol, *Angew. Chem., Int. Ed.*, 2015, **54**, 14858–14861.
- 14 (a) E. L. Whitelaw, G. Lorain, M. F. Mahon and M. D. Jones, *Dalton Trans.*, 2011, **40**, 11469–11473; (b) I. dos Santos Vieira, E. L. Whitelaw, M. D. Jones and S. Herres-Pawlis, *Chem. – Eur. J.*, 2013, **19**, 4712–4716; (c) S. L. Hancock, M. F. Mahon and M. D. Jones, *Dalton Trans.*, 2013, **42**, 9279–9285; (d) A. Pilone, K. Press, I. Goldberg, M. Kol, M. Mazzeo and M. Lamberti, *J. Am. Chem. Soc.*, 2014, **136**, 2940–2943.
- 15 (a) N. Nomura, T. Aoyama, R. Ishii and T. Kondo, *Macromolecules*, 2005, **38**, 5363–5366; (b) J. Liu, N. Iwasa and K. Nomura, *Dalton Trans.*, 2008, 3978–3988; (c) D. Pappalardo, L. Annunziata and C. Pellicchia, *Macromolecules*, 2009, **42**, 6056–6062; (d) W. Zhang, Y. Wang, W.-H. Sun, L. Wang and C. Redshaw, *Dalton Trans.*, 2012, **41**, 11587–11596; (e) A. Meduri, T. Fuoco, M. Lamberti, C. Pellicchia and D. Pappalardo, *Macromolecules*, 2014, **47**, 534–543.

- 16 (a) S. Gong and H. Ma, *Dalton Trans.*, 2008, 3345–3357; (b) W. Yai, Y. Mu, A. Gao, W. Gao and L. Ye, *Dalton Trans.*, 2008, 3199–3206; (c) D. Li, Y. Peng, C. Geng, K. Liu and D. Kong, *Dalton Trans.*, 2013, **42**, 11295–11303; (d) D.-R. Dauer and D. Stalke, *Dalton Trans.*, 2014, **43**, 14432–14439.
- 17 (a) F. Qian, K. Liu and H. Ma, *Dalton Trans.*, 2010, **39**, 8071–8083.
- 18 (a) W. Zhang, Y. Wang, L. Wang, C. Redshaw and W.-H. Sun, *J. Organomet. Chem.*, 2014, **750**, 65–73; (b) J. Liu and H. Ma, *J. Polym. Sci., Part A: Polym. Chem.*, 2014, **52**, 3096–3106; (c) T.-L. Huang and C.-T. Chen, *J. Organomet. Chem.*, 2013, **725**, 15–21; (d) L. Postigo, M. D. C. Maestra, M. E. G. Mosquera, T. Cuenca and G. Jiménez, *Organometallics*, 2013, **32**, 2618–2624; (e) S. Bian, S. Abbina, Z. Lu, E. Kolodka and G. Du, *Organometallics*, 2014, **33**, 2489–2495; (f) M. Bouyahyi, T. Roisnel and J.-F. Carpentier, *Organometallics*, 2012, **31**, 1458–1466; (g) A. Gao, Y. Mu, J. Zhang and W. Yao, *Eur. J. Inorg. Chem.*, 2009, 3613–3621; (h) R.-C. Yu, C.-H. Hung, J.-H. Huang, H.-Y. Lee and J.-T. Chen, *Inorg. Chem.*, 2002, **41**, 6450–6455.
- 19 (a) S. Tabthong, T. Nanok, P. Kongsaree, S. Prabpai and P. Hormnirun, *Dalton Trans.*, 2014, **43**, 1348–1359; (b) S. Pracha, S. Praban, A. Niewpung, G. Kotpisan, P. Kongsaree, S. Saitong, T. Khamnaen, P. Phiriyawirut, S. Charoenchaidet and K. Phomphrai, *Dalton Trans.*, 2013, **42**, 15191–15198.
- 20 C.-Y. Li, D.-C. Liu and B.-T. Ko, *Dalton Trans.*, 2013, **42**, 11488–11496.
- 21 (a) C.-H. Huang, F.-C. Wang, B.-T. Ko, T.-L. Yu and C.-C. Lin, *Macromolecules*, 2001, **34**, 356–361; (b) M. Shen, W. Huang, W. Zhang, X. Hao, W.-H. Sun and C. Redshaw, *Dalton Trans.*, 2010, **39**, 9912–9922; (c) N. Ikpo, S. M. Barbon, M. W. Drover, L. N. Dawe and F. M. Kerton, *Organometallics*, 2012, **31**, 8145–8158.
- 22 (a) R. Czerwieńiec, A. Kapturkiewicz, R. Anulewicz-Ostrowska and J. Nowacki, *J. Chem. Soc., Dalton Trans.*, 2002, 3434–3441; (b) T. E. Keyes, D. Leane, R. J. Forster, C. G. Coates, J. J. McGarvey, M. N. Nieuwenhuyzen, E. Figgemeier and J. G. Vos, *Inorg. Chem.*, 2002, **41**, 5721–5732; (c) Y.-P. Toong, S.-L. Zheng and X.-M. Chen, *Inorg. Chem.*, 2005, **44**, 4270–4275; (d) Y. You, J. Seo, S. H. Kim, K. S. Kim, T. K. Ahn, D. Kim and S. Y. Park, *Inorg. Chem.*, 2008, **47**, 1476–1487; (e) M. A. Kathova, T. V. Balashova, V. A. Llichev, A. N. Konev, N. A. Isachenkov, G. K. Fukin, S. Y. Ketkov and M. N. Bochkarev, *Inorg. Chem.*, 2010, **49**, 5094–5100; (f) Y. Liu, M. Li, Q. Zhao, H. Wu, K. Huang and F. Li, *Inorg. Chem.*, 2011, **50**, 5969–5977.
- 23 X.-C. Shi and G.-X. Jin, *Dalton Trans.*, 2011, **40**, 11914–11919.
- 24 X.-C. Shi and G.-X. Jin, *Organometallics*, 2012, **31**, 7198–7205.
- 25 (a) J. Massue, D. Frath, G. Ulrich, P. Retailleau and R. Ziessel, *Org. Lett.*, 2012, **14**, 230–233; (b) J. Chang, K. Zhao and S. Pan, *Tetrahedron Lett.*, 2002, **43**, 951–954.
- 26 (a) D. A. Atwood and M. J. Harvey, *Chem. Rev.*, 2001, **101**, 37–52; (b) R. Benn, A. Ruffinska, H. Lehmkuhl, E. Janssen and C. Krüger, *Angew. Chem., Int. Ed. Engl.*, 1983, **22**, 779–780; (c) R. Benn and A. Ruffinska, *Angew. Chem., Int. Ed. Engl.*, 1986, **25**, 861–881.
- 27 (a) C. E. Radzewich, M. P. Coles and R. F. Jordon, *J. Am. Chem. Soc.*, 1998, **120**, 9384–9385; (b) C. E. Radzewich, I. A. Guzei and R. F. Jordon, *J. Am. Chem. Soc.*, 1999, **121**, 8673–8674; (c) N. Iwasa, S. Katao, J. Liu, M. Fujiki, Y. Furukawa and K. Nomura, *Organometallics*, 2009, **28**, 2179–2187; (d) S. Gong and H. Ma, *Dalton Trans.*, 2008, 3345–3357; (e) Z. Zhong, P. J. Dijkstra and J. Feijen, *Angew. Chem., Int. Ed.*, 2002, **41**, 4510–4513.
- 28 The τ value ranges from 0 (perfectly square pyramidal) to 1 (perfectly trigonal bipyramidal). (a) A. W. Addison, T. N. Rao, J. Reedijk, J. van Rijn and G. C. Verschoor, *J. Chem. Soc., Dalton Trans.*, 1984, 1349–1356; (b) M.-A. Munoz-Hernandez, T. S. Keizer, P. Wei, S. Parkin and D. A. Atwood, *Inorg. Chem.*, 2001, **40**, 6782–6787.
- 29 (a) I. Barakat, Ph. Dubois, R. Jérôme and Ph. Teyssié, *J. Polym. Sci., Part A: Polym. Chem.*, 1993, **31**, 505–514; (b) J. Baran, A. Duda, A. Kowalski, R. Szymanski and S. Penczek, *Macromol. Rapid Commun.*, 1997, **18**, 325–333; (c) A. Kowalski, A. Duda and S. Penczek, *Macromolecules*, 1998, **31**, 2114–2122.
- 30 (a) A. Amgoune, C. M. Thomas and J.-F. Carpentier, *Macromol. Rapid Commun.*, 2007, **28**, 693–697; (b) M. Helou, O. Miserque, J.-M. Brusson, J.-F. Carpentier and S. M. Guillaume, *Chem. – Eur. J.*, 2008, **14**, 8772–8775; (c) C. Guillaume, J.-F. Capentier and S. M. Guillaume, *Polymer*, 2009, **50**, 5909–5917; (d) N. Ajellal, J.-F. Carpentier, C. Guillaume, S. M. Guillaume, M. Helou, V. Poirier, Y. Sarazin and A. Trifonov, *Dalton Trans.*, 2010, **39**, 8363–8376; (e) S. Qiao, W.-A. Ma and Z.-X. Wang, *J. Organomet. Chem.*, 2011, **696**, 2746–2753; (f) H.-J. Chuang, Y.-C. Su, B.-T. Ko and C.-C. Lin, *Inorg. Chem. Commun.*, 2012, **18**, 38–42; (g) K. D. Rebecca, A. M. Reckling, H. Chen, L. N. Dawe, C. M. Schneider and C. M. Kozak, *Dalton Trans.*, 2013, **42**, 3504–3520; (h) F. Hild, N. Neehaul, F. Bier, M. Wirsum, C. Gourlaouen and S. Dagorne, *Organometallics*, 2013, **32**, 587–598; (i) C.-H. Wang, C.-Y. Li, B.-H. Huang, C.-C. Lin and B.-T. Ko, *Dalton Trans.*, 2013, **42**, 10875–10884.
- 31 P. A. Cameron, D. Jhurry, V. C. Gibson, A. J. P. White, D. J. Williams and S. Williams, *Macromol. Rapid Commun.*, 1999, **20**, 616–618.
- 32 (a) C. K. A. Gregson, I. J. Blackmore, V. C. Gibson, N. J. Long, E. L. Marshall and A. J. P. White, *Dalton Trans.*, 2006, 3134–3140; (b) J. Wu, Y.-Z. Chen, W.-C. Hung and C.-C. Lin, *Organometallics*, 2008, **27**, 4970–4978.
- 33 K. Dink, M. O. Miranda, B. Moscato-Goodpaster, N. Ajellal, L. E. Breyfogle, E. D. Hermes, C. P. Schaller, S. E. Roe, C. J. Cramer, M. A. Hillmyer and W. B. Tolman, *Macromolecules*, 2012, **45**, 5387–5396.
- 34 (a) K. A. M. Thakur, R. T. Kean, E. S. Hall, J. J. Kolstad, T. A. Lindgren, M. A. Doscotch, J. I. Siepmann and E. J. Munson, *Macromolecules*, 1997, **30**, 2422–2428; (b) K. A. M. Thakur, R. T. Kean, E. S. Hall, J. J. Kolstad and E. J. Munson, *Macromolecules*, 1998, **31**, 1487–1494;

- (c) K. A. M. Thakur, R. T. Kean, M. T. Zell, B. E. Padden and E. J. Munson, *Chem. Commun.*, 1998, 1913–1914; (d) M. H. Chisholm, S. S. Iyer, D. G. McCollum, M. Pagel and U. Werner-Zwanziger, *Macromolecules*, 1999, **32**, 963–973; (e) M. T. Zell, B. E. Padden, A. J. Paterick, K. A. Thakur, R. T. Kean, M. A. Hillmyer and E. J. Munson, *Macromolecules*, 2002, **35**, 7700–7707; (f) J. Coudane, C. Ustariz-Peyret, G. Schwach and M. Vert, *J. Poly. Sci., Part A: Polym. Chem.*, 1997, **35**, 1651–1658.
- 35 M. Save, M. Schappacher and A. Soum, *Macromol. Chem. Phys.*, 2002, **203**, 889–899.
- 36 S. Matsui, M. Mitani, J. Saito, Y. Tohi, H. Makio, N. Matsukawa, Y. Takagi, K. Tsuru, M. Nitabaru, T. Nakano, H. Tanaka, N. Kashiwa and T. Fujita, *J. Am. Chem. Soc.*, 2001, **123**, 6847–6856.
- 37 H. E. Gottlieb, B. Kotlyar and A. Nudelman, *J. Org. Chem.*, 1997, **62**, 7512–7515.
- 38 M. C. Burla, R. Caliandro, M. Camalli, B. Carrozzini, G. L. Cascarano, L. De Caro, C. Giacovazzo, G. Polidori, D. Siliqi and R. Spagna, *J. Appl. Crystallogr.*, 2007, **40**, 609–613.
- 39 L. J. Bourhis, O. V. Dolomanov, R. J. Gildea, J. A. K. Howard and H. Puschmann, *Acta Crystallogr., Sect. A: Found. Crystallogr.*, 2015, **71**, 59–75.
- 40 G. M. Sheldrick, *Acta Crystallogr., Sect. A: Found. Crystallogr.*, 2015, **71**, 3–8.
- 41 G. M. Sheldrick, *Acta Crystallogr., Sect. A: Found. Crystallogr.*, 2015, **64**, 112–122.
- 42 O. V. Dolomanov, L. J. Bourhis, R. J. Gildea, J. A. K. Howard and H. Puschmann, *J. Appl. Crystallogr.*, 2009, **42**, 339–341.